© 2018. Published by The Company of Biologists Ltd | Development (2018) 145, dev161497. doi:10.1242/dev.161497

RESEARCH ARTICLE

Nkx genes establish second heart field cardiomyocyte progenitors at the arterial pole and pattern the venous pole through Isl1 repression

Sophie Colombo[1], Carmen de Sena-Tomás[1], Vanessa George[1], Andreas A. Werdich[2], Sunil Kapur[2], Calum A. MacRae[2] and Kimara L. Targoff[1,*]

ABSTRACT

NKX2-5 is the most commonly mutated gene associated with human congenital heart defects (CHDs), with a predilection for cardiac pole abnormalities. This homeodomain transcription factor is a central regulator of cardiac development and is expressed in both the first and second heart fields (FHF and SHF). We have previously revealed essential functions of *nkx2.5* and *nkx2.7*, two *Nkx2-5* homologs expressed in zebrafish cardiomyocytes, in maintaining ventricular identity. However, the differential roles of these genes in the specific subpopulations of the anterior (aSHF) and posterior (pSHF) SHFs have yet to be fully defined. Here, we show that Nkx genes regulate aSHF and pSHF progenitors through independent mechanisms. We demonstrate that Nkx genes restrict proliferation of aSHF progenitors in the outflow tract, delimit the number of pSHF progenitors at the venous pole and pattern the sinoatrial node acting through Isl1 repression. Moreover, optical mapping highlights the requirement for Nkx gene dose in establishing electrophysiological chamber identity and in integrating the physiological connectivity of FHF and SHF cardiomyocytes. Ultimately, our results may shed light on the discrete errors responsible for *NKX2-5*-dependent human CHDs of the cardiac outflow and inflow tracts.

KEY WORDS: *nkx2.5*, *nkx2.7*, Arterial pole, Venous pole, Second heart field, Zebrafish

INTRODUCTION

Cardiomyocytes (CMs) are derived from at least two distinct cardiac progenitor populations located in the splanchnic mesoderm. First heart field (FHF) cells differentiate early in the lateral plate mesoderm to give rise to the linear heart tube (Buckingham et al., 2005; Vincent and Buckingham, 2010). Subsequently, second heart field (SHF) cells migrate to the pharyngeal mesoderm, proliferate and differentiate into CMs at the arterial and venous poles. The anterior SHF (aSHF) subpopulation gives rise to the right ventricle and outflow tract (OFT), whereas the posterior SHF (pSHF) contributes primarily to the atria and inflow tract (IFT) (Buckingham et al., 2005; Cai et al., 2003; Dominguez et al., 2012; Dyer and Kirby, 2009; Galli et al., 2008; Rana et al., 2014; Vincent and Buckingham, 2010; Zaffran et al., 2004). Errors in specification and differentiation of the SHF cells under these precise spatial and temporal constraints can lead to a variety of congenital heart defects (CHDs), specifically conotruncal (OFT) and atrial (IFT) abnormalities. These malformations of the cardiac poles are found in 10% and 30%, respectively, of individuals with CHDs and result in significant neonatal morbidity and mortality (Gelb and Chung, 2014; Hoffman and Kaplan, 2002; Hoffman et al., 2004; Loffredo, 2000; Nemer, 2008; Payne et al., 1995; Pierpont et al., 2007; Supino et al., 2006). Despite this clinical impact, the mechanisms underlying the development of the arterial and venous poles of the heart are incompletely understood.

NKX2-5, a homeodomain transcription factor expressed in cells of the FHF and SHF (Stanley et al., 2002), and a regulator of cardiac development (Bruneau, 2008), is associated with a myriad of human CHDs. Moreover, individuals carrying *NKX2-5* mutations demonstrate a propensity to develop malformations involving the poles of the heart, such as Tetralogy of Fallot, double outlet right ventricle and atrial septal defects (Abou Hassan et al., 2015; Benson et al., 1999; Chung and Rajakumar, 2016; Elliott et al., 2003; Goldmuntz et al., 2001; McElhinney et al., 2003; Nakajima, 2010; Schott et al., 1998; Srivastava and Olson, 2000). Investigation of the genetic basis of CHDs in model systems has yielded insights into functions of *Nkx2-5* in progenitor specification in *Drosophila*, *Xenopus* and mouse (Azpiazu and Frasch, 1993; Bodmer, 1993; Grow and Krieg, 1998; Prall et al., 2007), and in cardiac morphogenesis in mouse and zebrafish (Barth et al., 2010; Lyons et al., 1995; Prall et al., 2007; Tanaka et al., 1999; Targoff et al., 2013, 2008; Tu et al., 2009). Furthermore, *Nkx2-5* mutants, whether inside or outside the DNA-binding domains (Benson et al., 1999; Gutierrez-Roelens et al., 2002; Ikeda et al., 2002), regulate wild-type targets and also 'off-targets', destabilizing the cardiac transcriptional hierarchy in this context (Bouveret et al., 2015). Although previous work has revealed specific roles for *Nkx2-5* in the SHF (Cambier et al., 2014; Clark et al., 2013; Dorn et al., 2014; George et al., 2015; Guner-Ataman et al., 2013; Prall et al., 2007; Watanabe et al., 2012; Witzel et al., 2012; Zhang et al., 2014), the distinct cellular and molecular mechanisms operating in the aSHF and pSHF subpopulations remain largely unknown.

Recent studies have revealed essential functions of Nkx2-5 transcriptional regulation in OFT development. In mouse, Nkx2-5 has been shown to drive arterial pole formation via a Bmp2/Smad1 negative-feedback loop (Prall et al., 2007) and through a direct repressive effect on a 1.7 kb Fgf10 enhancer element (Watanabe et al., 2012). In zebrafish, *nkx2.5* plays a role in aSHF proliferation (Guner-Ataman et al., 2013) and stabilization of Nkx2.5 by Ajuba protein regulates progenitor specification in this population (Witzel et al., 2012). Moreover, the expression patterns of *ltbp3* and *mef2cb*,

[1]Division of Cardiology, Department of Pediatrics, College of Physicians and Surgeons, Columbia University, New York, NY 10032, USA. [2]Brigham and Women's Hospital/Harvard Medical School, Cardiovascular Division, 75 Francis Street, Thorn 11, Boston, MA 02115, USA.

*Author for correspondence (kl284@columbia.edu)

S.C., 0000-0001-8945-5631; V.G., 0000-0003-1990-4651; A.A.W., 0000-0002-1222-1180; C.A.M., 0000-0001-5181-2664; K.L.T., 0000-0002-6066-6002

Received 16 November 2017; Accepted 4 December 2017

Development (2018) 145, dev161497. doi:10.1242/dev.161497

aSHF markers in zebrafish, overlap with the *nkx2.5*-expressing region near the arterial pole (Lazic and Scott, 2011; Zhou et al., 2011). Although these data document the importance of Nkx genes in arterial pole development, it is unclear how Nkx2.5 controls differentiation and expansion of the aSHF progenitor pool to sculpt the precise dimensions of the OFT.

At the sinus venosus (SV), extensive studies have elucidated the function of *Nkx2-5* in cardiac conduction system (CCS) development (Briggs et al., 2008; Jay et al., 2004; Moskowitz et al., 2007; Nakashima et al., 2009; Pashmforoush et al., 2004; Ye et al., 2015). Yet the mechanisms by which Nkx genes direct pSHF progenitors to pattern the venous pole have not been fully defined. It is evident from murine models that pSHF cells accumulate in the atrial chambers (Cai et al., 2003; Galli et al., 2008; Lescroart et al., 2012) and pSHF progenitors direct the molecular and cellular events contributing to atrioventricular (AV) septation (Goddeeris et al., 2008; Hoffmann et al., 2009, 2014; Mommersteeg et al., 2006; Snarr et al., 2007a,b; Xie et al., 2012). Interestingly, Nkx2-5 is important in establishing a balance between sinoatrial node (SAN) and atrial myocardial identities (Espinoza-Lewis et al., 2011; Mommersteeg et al., 2007; Nakashima et al., 2014). Another homeodomain transcription factor, Shox2, is also essential for SAN development, in part through repression of Nkx2-5 (Blaschke et al., 2007; Espinoza-Lewis et al., 2009). This Shox2-Nkx2-5 antagonistic mechanism inhibits pacemaker properties that define a 'default' primitive cellular phenotype (Ye et al., 2015). Furthermore, studies have shown that Shox2 directly regulates Isl1 (Hoffmann et al., 2013) and Nkx2-5 inhibits *Isl1* (Dorn et al., 2014; Prall et al., 2007; Watanabe et al., 2012), a key cardiac transcription factor expressed in the pSHF (Cai et al., 2003; Snarr et al., 2007a; Sun et al., 2007; van den Berg et al., 2009). Variation in ISL1 confers genetic susceptibility for CHDs (Stevens et al., 2010), thus highlighting a crucial role in human disease. Moreover, data have illuminated a pivotal role for *Isl1* in SAN development and function (Liang et al., 2015; Tessadori et al., 2012; Vedantham et al., 2015), and these findings offer explanations for CCS abnormalities in individuals harboring *NKX2-5* mutations. Given embryonic stem cell work suggesting that direct Isl1 repression by Nkx2-5 is necessary to establish the ventricular lineage (Dorn et al., 2014) and our findings revealing essential roles of Nkx genes in ventricular identity maintenance (George et al., 2015; Targoff et al., 2013), we sought to uncover novel Nkx-Isl1 interactions that are required to pattern the IFT.

Our previous studies demonstrate that the *Nkx2-5* homologs expressed in zebrafish CMs, *nkx2.5* and *nkx2.7* (Lee et al., 1996), act redundantly in cardiac morphogenesis (Targoff et al., 2008; Tu et al., 2009) and are crucial in maintaining ventricular identity by repressing atrial fate (Targoff et al., 2013). Furthermore, temporally controlled expression of *nkx2.5* is essential to ensure chamber-specific identity maintenance in both the FHF and SHF during explicit developmental time windows (George et al., 2015). Despite these insights, little is known about the mechanisms by which Nkx genes control the specification and differentiation of SHF progenitors at the cardiac poles. In this study, we find that Nkx genes positively regulate aSHF progenitors at the arterial pole and restrict pSHF-derived CM differentiation at the venous pole. At the arterial pole, Nkx genes are required to promote the aSHF progenitors, within the proliferating pharyngeal region, to differentiate and assemble the OFT. In *nkx2.5*$^{-/-}$;*nkx2.7*$^{-/-}$ embryos, unrestricted expression patterns of SAN genes, *bmp4*, *tbx2b*, *hcn4* and *shox2*, highlight severe abnormalities in venous pole development. Furthermore, our findings reveal that Nkx genes normally restrict *isl1* expression to the venous pole during heart tube formation, whereas overexpression of *nkx2.5* is sufficient to inhibit *isl1*. Notably, electrophysiological chamber identity is dependent on Nkx gene dose with elimination of all heterogeneity of intercellular coupling in the *nkx2.5*$^{-/-}$;*nkx2.7*$^{-/-}$ embryos. These findings support the innovative concept that CM differentiation is highly graded, with functional partitioning of the heart tube established and maintained through networks of overlapping regulators rather than through binary fate choices. This gradation is consistent with the pleiotropy of phenotypes observed in monogenic forms of CHD and the known redundancy and resilience of cardiac transcriptional networks. Taken together, our results suggest key functions of Nkx genes in SHF CM differentiation in mediating differential roles in anterior and posterior populations. Ultimately, our studies have the potential to shed light on the mechanisms underlying conotruncal and venous pole malformations, and conduction system defects in individuals carrying *NKX2-5* mutations.

RESULTS

OFT size is restricted in *nkx* mutants

Although our previous studies revealed synergistic functions of *nkx2.5* and *nkx2.7* in OFT development (George et al., 2015; Targoff et al., 2013), the discrete cellular and temporal mechanisms operating downstream of Nkx genes in the aSHF remain unclear. Previous studies have identified SHF progenitors in the anterior lateral plate mesoderm (ALPM) that express *nkx2.5* and contribute to the OFT (Guner-Ataman et al., 2013; Paffett-Lugassy et al., 2017). Thus, we examined the roles of *nkx2.5* and *nkx2.7* in regulating the spatiotemporal contribution of the aSHF to arterial pole formation. Employing a developmental timing assay to assess the differences in protein maturation time in embryos expressing *Tg(myl7:EGFP)* and *Tg(-5.1myl7:nDsRed2)* (de Pater et al., 2009; Huang et al., 2003; Mably et al., 2003) (Fig. 1A-I), we visualized the accretion of the aSHF-derived CMs in the OFT of wild-type and *nkx2.5*$^{-/-}$; *nkx2.7*$^{+/+}$, *nkx2.5*$^{-/-}$; *nkx2.7*$^{+/-}$ and *nkx2.5*$^{-/-}$; *nkx2.7*$^{-/-}$ (hereafter referred to as *nkx* mutant) embryos. Progressive loss of Nkx gene function highlights substantial reduction in the volume of OFT myocardium (Fig. 1D-I). Moreover, we detected a statistically significant reduction in aSHF-derived CMs, or EGFP^{+} DsRed^{-} cells, when comparing wild-type (24 cells±3 cells; n=12) with *nkx2.5*$^{-/-}$;*nkx2.7*$^{-/-}$ (16 cells±4 cells; n=3) embryos (P<0.005). Taken together, these findings underscore that *nkx2.5* and *nkx2.7* positively regulate the contribution of aSHF progenitors at the zebrafish arterial pole.

Nkx genes are dispensable for OFT cardiomyocyte proliferation

Prior work has elucidated an important role for SHF CM proliferation in zebrafish arterial pole development (Guner-Ataman et al., 2013; Lazic and Scott, 2011; Nevis et al., 2013; Schindler et al., 2014; Zeng and Yelon, 2014; Zhou et al., 2011). Given the decreased number of aSHF-derived CMs in the *nkx* mutant OFT, we tested whether diminished proliferation is responsible for this observation. We pulsed embryos carrying *Tg(-5.1myl7:nDsRed2)* at 24 hpf, when aSHF-derived CMs proliferate, with the thymidine analog 5-ethynyl-2′-deoxyuridine (EdU) (Guner-Ataman et al., 2013; Schindler et al., 2014; Zeng and Yelon, 2014). At 48 hpf, we counted EdU^{+} DsRed^{+} MF20^{+} cells at the arterial pole to quantify proliferating nuclei in the myocardium (Fig. S1). We detected no statistically significant differences in the proliferation indices between wild-type (1.0%±1.3%; n=15) and

Development (2018) 145, dev161497. doi:10.1242/dev.161497

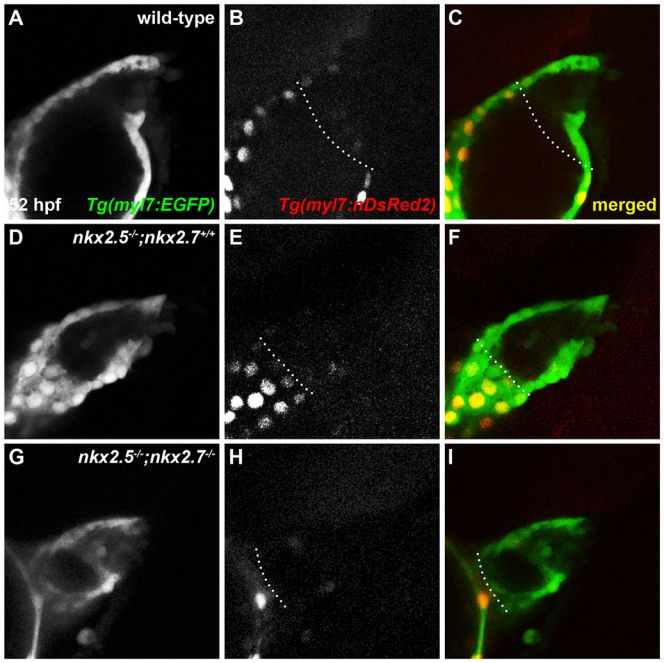

Fig. 1. OFT size and CM numbers are reduced in *nkx* mutants. (A-I) Lateral view, anterior towards the right, at 52 hpf. Representative reconstructions of four *z*-stacks from a developmental timing assay show diminished cell numbers in the OFT of wild-type (A-C), *nkx2.5*$^{-/-}$;*nkx2.7*$^{+/+}$ (D-F) and *nkx2.5*$^{-/-}$;*nkx2.7*$^{-/-}$ (G-I) embryos carrying *Tg(myl7:EGFP)* and *Tg(-5.1myl7:nDsRed2)*.

nkx mutant (1.5%±1.2%; *n*=8) embryos, indicating that a reduced rate of OFT proliferation is not responsible for the decrease in CMs accrued at the arterial pole.

Nkx genes delimit the OFT progenitor pool

We then postulated that a shrunken arterial pole size in Nkx mutant embryos could represent an earlier influence of Nkx genes on the reservoir of undifferentiated aSHF progenitors. The SHF-derived population at the OFT can be divided into two cell types: differentiated CMs that strongly express *myl7*, *vmhc* and *nkx2.5*, and a progenitor pool that faintly expresses these same markers and strongly expresses *mef2cb* and *ltbp3* (Lazic and Scott, 2011; Zeng and Yelon, 2014; Zhou et al., 2011). Indeed, our findings reveal diminished *mef2cb* expression in the arterial pole of wild-type compared with *nkx* mutant embryos (Fig. 2A-E). Specifically, *mef2cb* expression is slightly decreased in *nkx2.5*$^{-/-}$;*nkx2.7*$^{+/+}$ and *nkx2.5*$^{-/-}$;*nkx2.7*$^{+/-}$ embryos (Fig. 2C,D), and further diminished in *nkx2.5*$^{-/-}$;*nkx2.7*$^{-/-}$ embryos (Fig. 2E) when compared with wild-type and *nkx2.5*$^{+/+}$;*nkx2.7*$^{-/-}$ embryos (Fig. 2A,B). These results corroborate our previously published studies illustrating a progressive decline in *ltbp3* expression with successive reduction of Nkx gene dose (Targoff et al., 2013). Altogether, our findings suggest that Nkx gene function is required to establish the proper size of the aSHF progenitor pool. However, in assessing this population through gene expression profiles of SHF markers, we may fail to identify all cells destined to become aSHF-derived CMs.

Given the importance of the temporal regulation of aSHF precursor accretion to the arterial pole (Cambier et al., 2014; Jahangiri et al., 2016; Zeng and Yelon, 2014), we sought to quantify aSHF progenitors by tracking these late-differentiating cells during OFT recruitment. Recent studies have confirmed the contribution of distal *Tg(nkx2.5:ZsYellow)*-expressing progenitor cells to the OFT myocardium using *Tg(nkx2.5:kaede)* (Guner-Ataman et al., 2013; Zeng and Yelon, 2014). Employing *Tg(nkx2.5:ZsYellow)* and *Tg(myl7:EGFP)*, we examined aSHF progenitor cells in the pharyngeal region distal to the arterial pole where they proliferate prior to differentiation and addition to heart (Hutson et al., 2010; Tirosh-Finkel et al., 2010; van den Berg et al., 2009; Zeng and Yelon, 2014). We observed dispersion and lower levels of expression of *Tg(nkx2.5:ZsYellow)* in the distal *nkx2.5*$^{+}$ OFT progenitors in *nkx* mutant compared with wild-type embryos at 36 hpf (Fig. 2F,G). We quantified this alteration in expression patterns by counting ZsYellow^{+} EGFP^{-} cells distal to the arterial pole and between the branchial arches (Fig. 2H). Our results demonstrate a dramatic decrease in the number of distal *nkx2.5*$^{+}$ progenitors contributing to the OFT in *nkx* mutant embryos. Together, these data suggest that loss of Nkx gene function limits the number of undifferentiated aSHF cells prior to their deployment to the arterial pole.

Nkx genes regulate OFT progenitor proliferation timing and differentiation

From our findings demonstrating that Nkx genes are required for OFT formation by early regulation of the aSHF progenitor pool size, as opposed to later influence on SHF-derived CM production, we postulated that the decreased number of OFT progenitors in Nkx mutants could be due to diminished progenitor proliferation. To investigate this hypothesis, we performed an EdU incorporation assay in embryos carrying *Tg(nkx2.5:ZsYellow)* at 18 hpf to identify dividing progenitor cells prior to their migration to the arterial pole. At 40 hpf, we performed MF20 immunostaining to delineate proliferative ZsYellow^{+} cells that had been incorporated into the OFT in wild-type (Fig. 3A,B) and *nkx* mutant (Fig. 3C,D) embryos. Surprisingly, we found no significant difference in the proliferation index of the total OFT progenitor population when comparing wild-type with *nkx* mutant embryos (Fig. 3E). We next tested whether there might be differences in OFT progenitor proliferation indices between wild-type and *nkx* mutant embryos in the proximal early-differentiating (ZsYellow^{+} MF20^{+}) and distal late-differentiating (ZsYellow^{+} MF20^{-}) populations. The proximal OFT progenitor population is recruited to the arterial pole while the distal OFT progenitor population remains in a proliferative state in the pharyngeal region (van den Berg et al., 2009). We found that our results from the EdU incorporation assay are comparable between wild-type and *nkx* mutant embryos in the proximal precursor population contributing to the arterial pole (Fig. 3F). However, there is a statistically significant increase in the proliferation index of those OFT progenitors that reside in the distal pharyngeal region when comparing wild-type and *nkx* mutant embryos (Fig. 3B compared with D; Fig. 3G). In summary, our data suggest that Nkx genes regulate OFT size by restricting the proliferation of aSHF progenitors in the distal pharyngeal region and promoting differentiation as they migrate to form the arterial pole.

isl1 functions downstream of Nkx genes at the venous pole

In light of our evidence suggesting that Nkx genes positively regulate the aSHF OFT progenitor pool, we examined possible roles in pSHF development given the relatively high incidence of atrial septal defects in individuals carrying *NKX2-5* mutations. In the absence of clearly defined regulators of the IFT in zebrafish, we investigated Isl1, a LIM homeodomain transcription factor, as a potential candidate downstream of Nkx genes at the venous pole. Extensive studies elucidated that *isl1* is essential for normal cardiac development across species (Brade et al., 2007; Cai et al., 2003; de

Development (2018) 145, dev161497. doi:10.1242/dev.161497

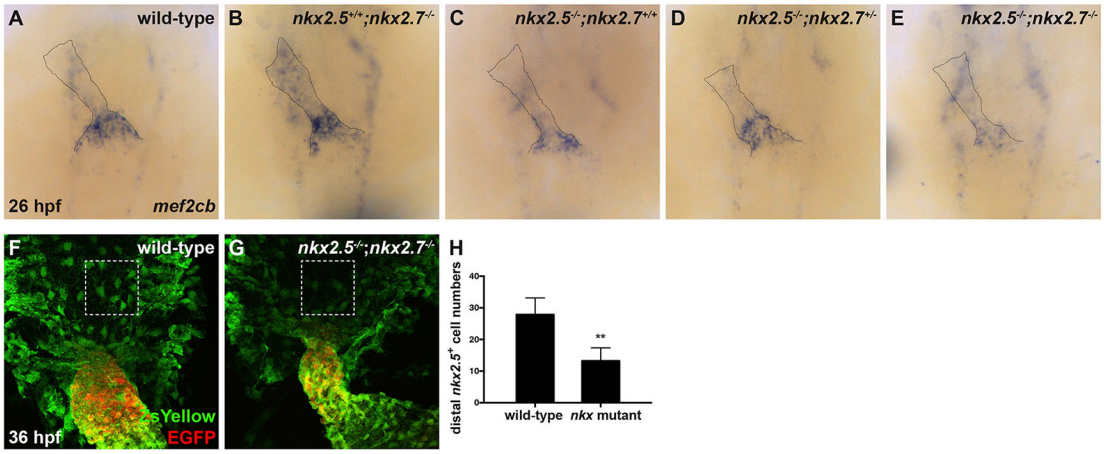

Fig. 2. Nkx genes delimit the OFT progenitor pool. (A-E) Dorsal view, anterior towards the top, at 26 hpf. *In situ* hybridization depicts diminished expression of *mef2cb*, which labels aSHF-derived CM progenitors, in representative *nkx2.5*$^{-/-}$;*nkx2.7*$^{+/+}$ (*n*=6) (C), *nkx2.5*$^{-/-}$;*nkx2.7*$^{+/-}$ (*n*=3) (D) and *nkx2.5*$^{-/-}$;*nkx2.7*$^{-/-}$ (*n*=5) (E) embryos compared with wild-type (*n*=15) (A) and *nkx2.5*$^{+/+}$;*nkx2.7*$^{-/-}$ (*n*=5) (B) embryos. (F,G) Ventral view of the arterial pole region at 36 hpf. Confocal projections of immunohistochemistry for ZsYellow (green) and EGFP (red) in embryos carrying *Tg(nkx2.5:ZsYellow)* and *Tg(myl7:EGFP)* illustrate decreased contribution of *nkx2.5*$^{+}$ aSHF-derived CM progenitors (ZsYellow^{+} EGFP^{-}) to the arterial pole in *nkx2.5*$^{-/-}$;*nkx2.7*$^{-/-}$ (G) compared with wild-type (F) embryos (boxed areas). (H) Quantification of ZsYellow^{+} EGFP^{-} cells at the arterial pole in wild-type (*n*=9) and *nkx* mutant (*n*=8) embryos reveals a statistically significant decrease in this population following the loss of Nkx gene function. Student's *t*-test was used to determine statistical significance. Mean and s.e.m. of each data set are shown (**P<0.0001).

Pater et al., 2009; Pandur et al., 2013; Witzel et al., 2012), delineates the SHF at both arterial and venous poles (Cai et al., 2003; Hami et al., 2011; Snarr et al., 2007a; Stoyek et al., 2015; Witzel et al., 2012), and is required for proper pacemaker development and function (Liang et al., 2015; Tessadori et al., 2012; Vedantham et al., 2015). In zebrafish, using an antibody that recognizes both Isl1 and Isl2 proteins (D'Amico et al., 2007; Hutchinson and Eisen, 2006; Witzel et al., 2012), Isl1/2^{+} cells are found near the OFT and IFT (de Pater et al., 2009; Hami et al., 2011; Witzel et al., 2012), and co-expression of Nkx2.5 in this population is evident during somitogenesis (Witzel et al., 2012). However, Isl2b appears to play a role in arterial pole development (Witzel et al., 2017) and Isl1 in venous pole development with a loss of late-differentiating CMs in the IFT in *isl1*$^{-/-}$ embryos (de Pater et al., 2009). Thus, we postulated that Nkx genes inhibit *isl1* expression at the SV. In support of our model, we found that Isl1 immunostaining is localized specifically to the IFT of wild-type embryos (Fig. 4A), while Isl1^{+} CMs extend throughout the atrium (S46^{+} region) in *nkx2.5*$^{-/-}$;*nkx2.7*$^{+/+}$ embryos (Fig. 4C) and reach the OFT in *nkx2.5*$^{-/-}$;*nkx2.7*$^{-/-}$ embryos (Fig. 4E). We quantified Isl1^{+} nuclei

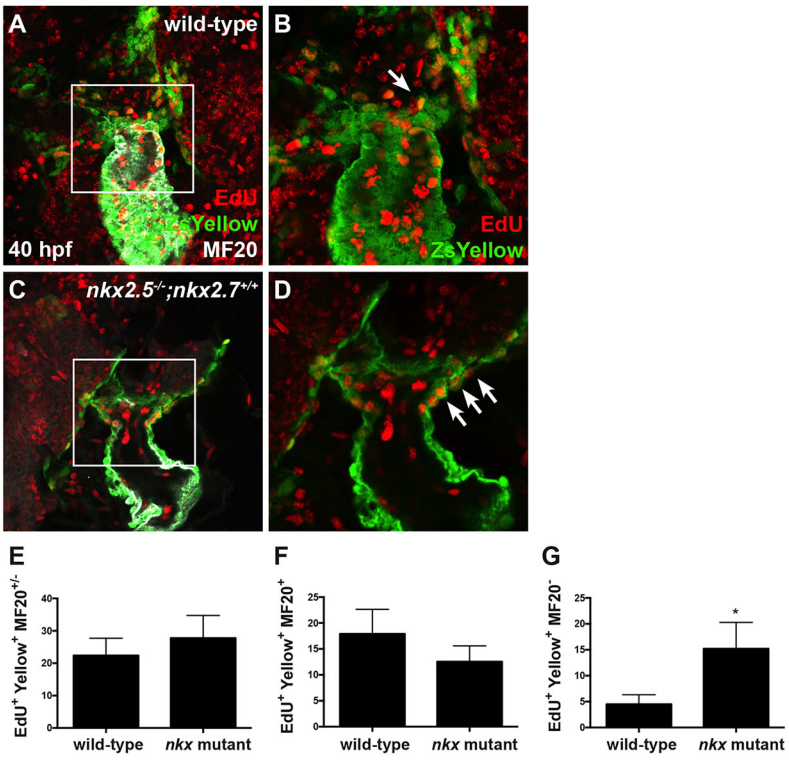

Fig. 3. Nkx genes regulate OFT progenitor proliferation timing and differentiation. (A-D) Ventral view of the arterial pole region at 40 hpf. Confocal projections of immunohistochemistry for EdU (red), ZsYellow (green) and MF20 (gray) in embryos carrying *Tg(nkx2.5:ZsYellow)* following EdU incubation at 18 hpf in wild-type (A,B) and *nkx2.5*$^{-/-}$;*nkx2.7*$^{+/+}$ (C,D) embryos. White arrows indicate EdU^{+} ZsYellow^{+} cells. The boxed areas in A,C are shown at higher magnification in B,D. (E-G) Proliferation indices showing a statistically significant increase in undifferentiated, ZsYellow^{+} MF20^{-} progenitors in *nkx* mutant (*n*=6) compared with wild-type (*n*=6) embryos (G); the proliferation index is comparable in the proximal, ZsYellow^{+} MF20^{+} CM population contributing to the arterial pole (F) as well as in the total OFT, ZsYellow^{+} MF20$^{+/-}$ CM population (E). Student's *t*-test was used to determine statistical significance. The mean and s.e.m. of each data set are shown (*P<0.005).

Development (2018) 145, dev161497. doi:10.1242/dev.161497

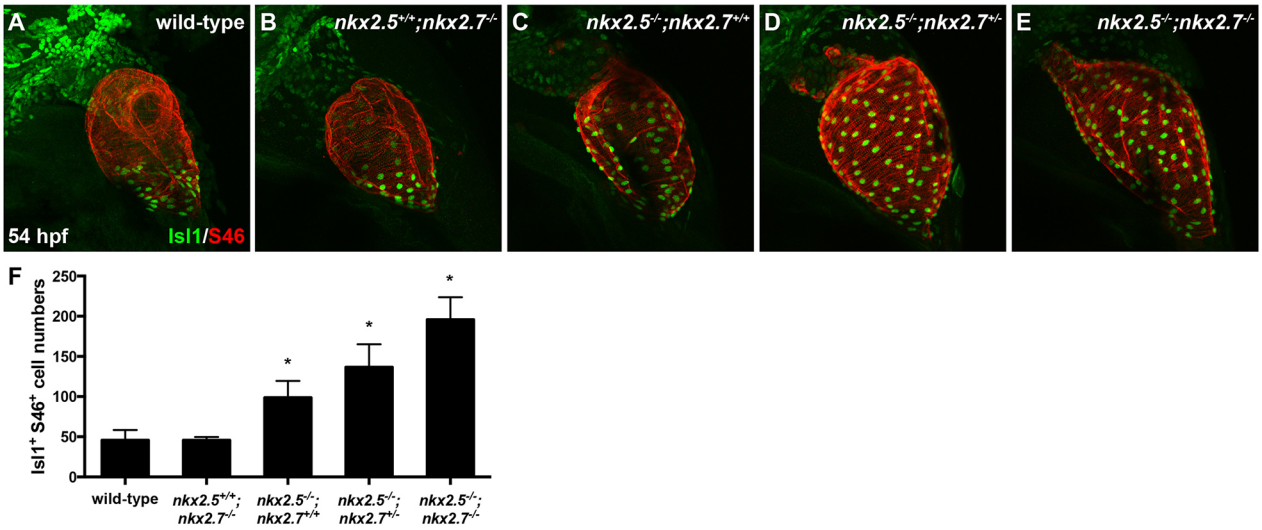

Fig. 4. Nkx genes inhibit Isl1 expression at the sinus venosus. (A-E) Lateral view, anterior towards the top, at 54 hpf in wild-type (A), *nkx2.5*$^{+/+}$;*nkx2.7*$^{-/-}$ (B), *nkx2.5*$^{-/-}$;*nkx2.7*$^{+/+}$ (C), *nkx2.5*$^{-/-}$;*nkx2.7*$^{+/-}$ (D) and *nkx2.5*$^{-/-}$;*nkx2.7*$^{-/-}$ (E) embryos. Representative confocal images of immunofluorescence for Isl1 (green) and S46 (red) demonstrate that Isl1 is restricted to the venous pole of wild-type (A) and *nkx2.5*$^{+/+}$;*nkx2.7*$^{-/-}$ (B) embryos. However, Isl1 expression expands throughout the atrium in *nkx* mutants (C-E). (F) Quantification of Isl1^{+} S46^{+} CMs is depicted showing a gradual increase in cell number with a progressive loss of *nkx* alleles. Mean and s.e.m. of each data set are shown (*P<0.005) in wild-type (n=16), *nkx2.5*$^{+/+}$;*nkx2.7*$^{-/-}$ (n=2), *nkx2.5*$^{-/-}$;*nkx2.7*$^{+/+}$ (n=6), *nkx2.5*$^{-/-}$;*nkx2.7*$^{+/-}$ (n=10) and *nkx2.5*$^{-/-}$;*nkx2.7*$^{-/-}$ (n=4) embryos. Student's t-test was used to determine statistical significance.

and detected a progressive increase in the number of cells expressing this transcription factor as Nkx gene dose is diminished (Fig. 4F). Notably, the number of Isl1^{+} CMs in the *nkx2.5*$^{-/-}$;*nkx2.7*$^{-/-}$ heart is approximately equivalent to the total number of CMs in wild-type embryos (Targoff et al., 2013). Next, we investigated Nkx2.5 and Isl1 expression patterns employing immunohistochemistry in embryos carrying *Tg(nkx2.5:ZsYellow)* at 52 hpf. This transgene faithfully recapitulates the endogenous *nkx2.5* expression observed by *in situ* hybridization (data not shown). We find that Nkx2.5 and Isl1 are virtually mutually exclusive at the venous pole in wild-type embryos (Fig. 5A-A″). Nkx2.5 is expressed in a decreasing gradient from the OFT to the inflow of the atrium, whereas Isl1 expression is confined to SV with only a few cells co-expressing Nkx2.5 and Isl1 (Fig. 5A″). Alternatively, in *nkx* mutants, Isl1 expression is derepressed in all atrial CMs that normally express Nkx2.5 (Fig. 5B-E″). Taken together, our studies strongly support the *in vivo* suppression of Isl1^{+} cell fate by Nkx genes in the SV during cardiac development.

We then explored the timing of the Nkx-Isl1 interaction in further detail. We evaluated *isl1* expression during early stages of cardiac differentiation in the ALPM. Our data illustrate that specification of *isl1*$^{+}$ progenitors occurs normally at 10 somites and 15 somites (Fig. 5F-I and data not shown), but *isl1* expression is enhanced at 26 hpf in *nkx* mutant compared with wild-type embryos (Fig. 5J-M). These findings indicate that Nkx genes are first required to inhibit *isl1* at the heart tube stage. Using a novel transgene generated in our lab for ubiquitous *nkx2.5* overexpression, *Tg(hsp70l:nkx2.5-EGFP)* (George et al., 2015), we tested the sufficiency of *nkx2.5* to inhibit *isl1* expression (Fig. 5N-Q). Following heat-shock activation of this inducible transgene at 21 somites, *isl1* expression was repressed specifically in the inflow region at both 24 hpf and 52 hpf (Fig. 5P,Q). Altogether, these results demonstrate that Nkx2.5 is not required for *isl1*$^{+}$ progenitor specification, but activation of Nkx2.5 transcription prior to heart tube elongation is sufficient to repress *isl1* at the venous pole during chamber emergence.

Nkx genes regulate differentiation of pSHF progenitors

Although recent work has shown the contribution of late-differentiating CMs to the venous pole in zebrafish (de Pater et al., 2009; Mosimann et al., 2015), little is known about the transcriptional regulatory networks guiding accretion and differentiation of this pSHF progenitor population. Given the ability of *nkx2.5* to restrict *Isl1* to the IFT (Fig. 5N-Q), we hypothesize that Nkx genes are essential in patterning the pSHF-derived CMs in this region. To test this hypothesis, we first performed a developmental timing assay to delineate the kinetics of pSHF progenitor accumulation using embryos expressing *Tg(myl7:EGFP)* and *Tg(-5.1myl7:nDsRed2)* (as in Fig. 1A-I). Intriguingly, our data reveal a statistically significant increase in pSHF-derived CMs, or EGFP^{+} DsRed^{-} CMs, at the venous pole in *nkx2.5*$^{-/-}$;*nkx2.7*$^{+/+}$ embryos along with further enhancement in *nkx2.5*$^{-/-}$;*nkx2.7*$^{-/-}$ embryos when compared with wild-type embryos (Fig. 6A-I,N). However, the source of the increased late-differentiating CMs at the IFT remains unknown. This finding may reflect either increased proliferation of pSHF progenitors or enhanced accrual of pSHF-derived CMs.

Consistent with our data illustrating normal CM production at the arterial pole following the loss of Nkx gene function (Fig. S1), we observed no difference in proliferation indices at the venous pole following EdU incorporation at 24 hpf between *nkx* mutant and wild-type embryos (data not shown). Thus, we hypothesized that Nkx genes are required for pSHF progenitor proliferation prior to accretion to the IFT. We performed an EdU incorporation assay at 18 hpf in embryos carrying *Tg(-5.1myl7:nDsRed2)* to detect dividing CMs at the venous pole. Quantification of the proliferation indices for EdU^{+} DsRed^{+} MF20^{+} cells in the IFT region at this time point also revealed no statistically significant difference between wild-type and *nkx* mutant embryos (Fig. 6J-M,O). These data support the conclusion that the IFT expansion in *nkx* mutant embryos is most likely due to enhanced pSHF-derived CM differentiation.

Development (2018) 145, dev161497. doi:10.1242/dev.161497

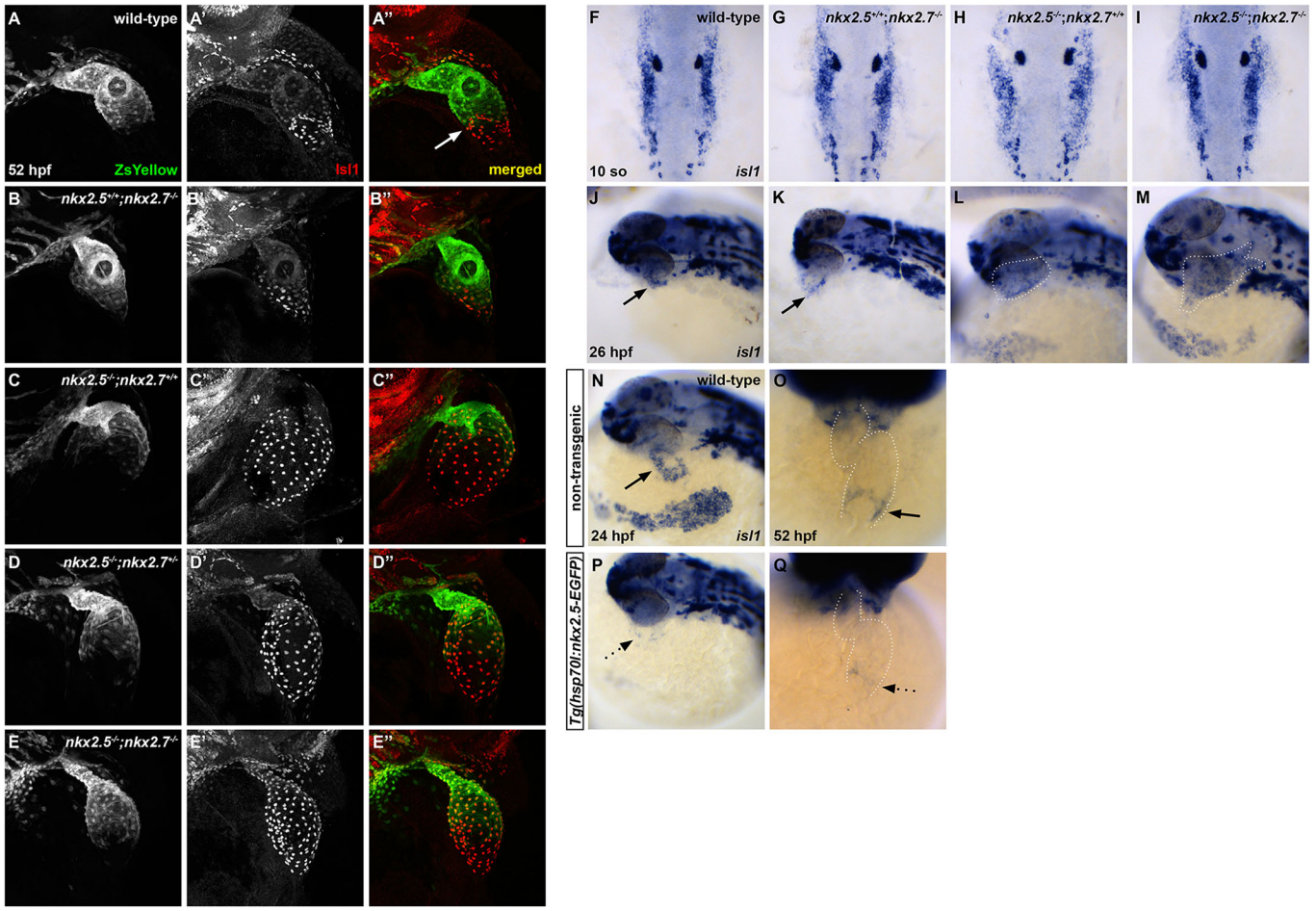

Fig. 5. Nkx2.5 is not required for *isl1*$^{+}$ progenitor specification, but is sufficient to repress *isl1* at the venous pole. (A-E″) Representative confocal images, lateral view, anterior towards the top, at 52 hpf. Immunostaining for Isl1 (red) in embryos carrying *Tg(nkx2.5:ZsYellow)* demonstrates that Isl1 is restricted to the venous pole and Nkx2.5 expression is absent in this region in wild-type (white arrow) (A-A″) and *nkx2.5*$^{+/+}$*;nkx2.7*$^{-/-}$ (B-B″) embryos. However, Isl1 expression is derepressed in the atrium of *nkx2.5*$^{-/-}$*;nkx2.7*$^{+/+}$ (C-C″) and *nkx2.5*$^{-/-}$*;nkx2.7*$^{+/-}$ (D-D″) embryos, and expands towards the outflow tract in *nkx2.5*$^{-/-}$*;nkx2.7*$^{-/-}$ (E-E″) embryos. (F-I) Dorsal view, anterior towards the top, at 10 somites. *In situ* hybridization shows no variation in ALPM *isl1* expression between wild-type (F) and *nkx* mutant (G-I) embryos. (J-M) Lateral view, anterior towards the left, at 26 hpf. *In situ* hybridization demonstrates that *isl1* expression is restricted to a ring at the venous pole of the heart tube in wild-type (J) and *nkx2.5*$^{+/+}$*;nkx2.7*$^{-/-}$ (K) embryos. However, *isl1* expression expands to the atrium in *nkx2.5*$^{-/-}$*;nkx2.7*$^{+/+}$ embryos (L) and throughout the entire heart tube in *nkx2.5*$^{-/-}$*;nkx2.7*$^{-/-}$ embryos (M). Black arrows indicate the ring of *isl1* expression near the IFT (J,K). (N-Q) Lateral view, anterior towards the left, at 24 hpf (N,P) and ventral view, anterior towards the top, at 52 hpf (O,Q) in non-transgenic (N,O) and *Tg(hsp70l:nkx2.5-EGFP)* (P,Q) embryos. *In situ* hybridization demonstrates that *isl1* expression is restricted to a ring at the venous pole (black arrows) at 24 hpf (*n*=9) (N) and 52 hpf (*n*=7) (O), and that overexpression of *nkx2.5* inhibits *isl1* expression specifically in this region (dotted arrows) at 24 hpf (*n*=9/11) (P) and 52 hpf (*n*=8/9) (Q).

Nkx genes pattern specialized nodal tissue in the sinus venosus via *isl1*

Although recent studies have elucidated the existence of specialized conduction tissue in the zebrafish heart (Arrenberg et al., 2010; Chi et al., 2008; Milan et al., 2006) and have identified *isl1*$^{+}$ as molecular marker of this population (Tessadori et al., 2012), the pathways controlling the development of the sinoatrial node (SAN) are still under investigation. Therefore, from evidence of conduction system abnormalities in individuals with *NKX2-5* mutations (Benson et al., 1999; Elliott et al., 2003; Gutierrez-Roelens et al., 2002; Schott et al., 1998) and from our findings revealing that Nkx genes regulate *isl1* expression (Figs 4 and 5), we posited that Nkx genes are fundamental in patterning the pSHF-derived CMs that contribute to the specialized nodal tissue in the SV. To address this issue, we explored the expression of a number of pacemaker cell genes: *bmp4*, *tbx2b, hcn4* and *shox2* (Blaschke et al., 2007; Espinoza-Lewis et al., 2009; Tessadori et al., 2012). In wild-type embryos, *bmp4*, *tbx2b* and *hcn4* expression is restricted to the OFT, atrioventricular canal (AVC) and IFT at 52 hpf (Fig. 7A,F,K). Intriguingly, all three genes are expressed throughout the myocardium in *nkx* mutant embryos (Fig. 7C-E,H-J,M-O). We observe a similar expression pattern for *shox2* when comparing wild-type and *nkx* mutant embryos (Fig. S2). Taken together, our findings illustrate that Nkx genes regulate regionalization of SAN markers to the IFT.

Next, we postulated that Isl1 acting downstream of Nkx genes is responsible for patterning the SAN and establishing the pacemaker activity of the zebrafish heart. Using a previously validated morpholino (MO) to knockdown Isl1 function (Hutchinson and Eisen, 2006), we observed that *bmp4* expression is absent in wild-type and *nkx2.5*$^{+/+}$*;nkx2.7*$^{-/-}$ embryos specifically at the IFT following *islet1E2* MO injection, whereas normal AVC and OFT expression of *bmp4* persists (compare Fig. 8A,B with F,G). These findings are consistent with evidence of selective inhibition of *bmp4* expression in the IFT of the *isl1*^{sa29} mutant (de Pater et al., 2009). Interestingly, inhibition of *isl1* splicing in *nkx* mutant embryos reveals specific downregulation of ectopic atrial and IFT *bmp4*

Development (2018) 145, dev161497. doi:10.1242/dev.161497

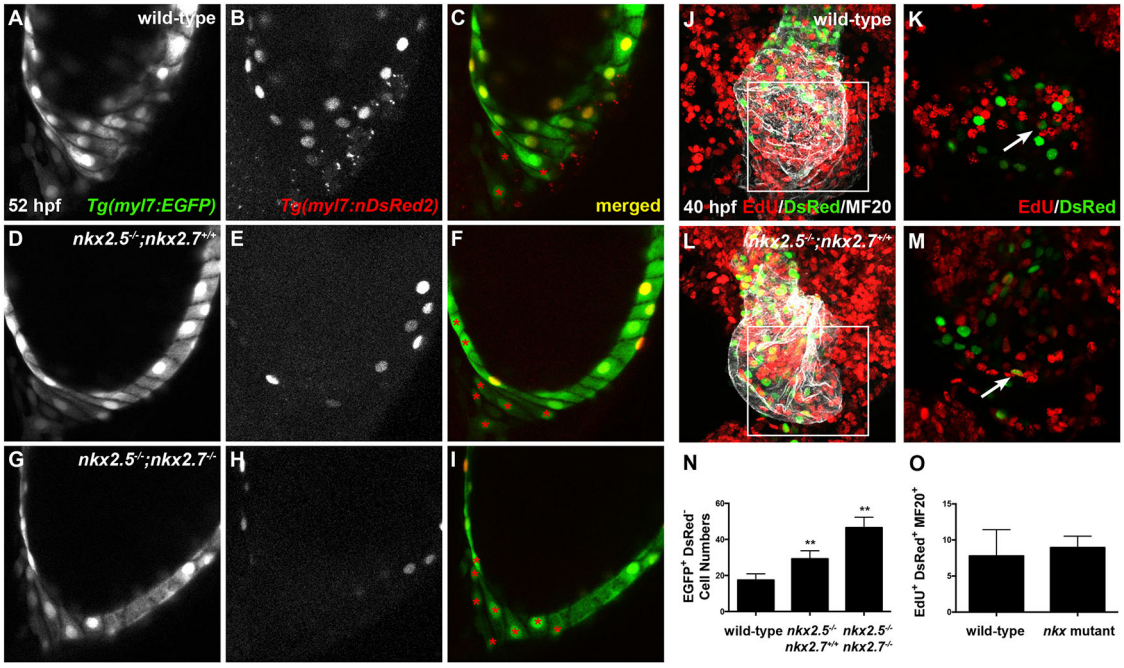

Fig. 6. Nkx genes regulate cardiomyocyte accretion to the atrium. (A-I) Lateral images, anterior towards the top, at 52 hpf. Representative reconstructions of 10 *z*-stacks from a developmental timing assay highlight the venous pole of wild-type (A-C), *nkx2.5*$^{-/-}$;*nkx2.7*$^{+/+}$ (D-F) and *nkx2.5*$^{-/-}$;*nkx2.7*$^{-/-}$ (G-I) embryos carrying *Tg(myl7:EGFP)* (green) and *Tg(-5.1myl7:nDsRed2)* (red). Asterisks indicate EGFP^{+} DsRed^{-} cells. (J-M) Ventral view, anterior towards the top, at 40 hpf of wild-type (J,K) and *nkx2.5*$^{-/-}$;*nkx2.7*$^{+/+}$ (L,M) embryos carrying *Tg(-5.1myl7:nDsRed2)*. Confocal projections (J,L) of immunohistochemistry for EdU (red), DsRed (green) and MF20 (gray) following EdU incubation at 18 hpf and four *z*-stack reconstructions (K,M) were used to count EdU^{+} DsRed^{+} MF20^{+} CMs in the atrium. The boxed areas in J,L are shown at higher magnification in K,M, respectively. White arrows indicate EdU^{+} DsRed^{+} CMs. (N,O) Quantification of EGFP^{+} DsRed^{-} cells at the venous pole for wild-type (*n*=12), *nkx2.5*$^{-/-}$;*nkx2.7*$^{+/+}$ (*n*=5) and *nkx2.5*$^{-/-}$;*nkx2.7*$^{-/-}$ (*n*=4) embryos, and proliferation indices in wild-type (*n*=5) and *nkx* mutant (*n*=3) embryos. Student's *t*-test was used to determine statistical significance. Mean and s.e.m. of each data set are shown (**P<0.0001). There is no statistically significant difference between proliferation indices in the DsRed^{+} MF20^{+} populations of wild-type and *nkx* mutant embryos.

expression (compare Fig. 8H-J with C-E) in the context of otherwise normal development. Together, our results demonstrate that the misregulation of *bmp4* expression in *nkx* mutant embryos is mediated by *isl1* overexpression, ultimately placing *isl1* downstream of Nkx genes in defining the pSHF-derived specialized conduction cells of the IFT.

Nkx genes regulate electrophysiological patterning

Finally, we explored the effects of the derepression of SAN genes on the electrophysiological phenotype in *nkx* mutant hearts. The establishment of electrical gradients enables the transition from peristaltic to sequential contraction in the developing heart and this patterning is regulated by differential contributions of FHF and SHF progenitor populations (Mosimann et al., 2015). We hypothesized that the loss of Nkx gene function could lead to a disruption in regional patterns of intercellular coupling given both the absence of ventricular identity (Targoff et al., 2013, 2008) and the expanded SAN gene expression domain in *nkx* mutant compared with wild-type embryos (Fig. 7).

To explore these issues, we measured action potential characteristics and conduction properties in isolated wild-type and *nkx* mutant hearts using high-resolution optical mapping (Fig. 9, Fig. S3). We did not detect any electrophysiological phenotypes in embryos carrying single-allele deficiencies in one or both *nkx* genes (*nkx2.5*$^{+/-}$;*nkx2.7*$^{+/+}$, *nkx2.5*$^{+/+}$;*nkx2.7*$^{+/-}$ and *nkx2.5*$^{+/-}$;*nkx2.7*$^{+/-}$). When comparing wild-type and *nkx2.5*$^{+/+}$;*nkx2.7*$^{-/-}$ embryos, there is no significant difference in the detailed action potential morphology (Fig. 9A,B), maximum upstroke velocity, $[dF/dt]_{max}$ (Fig. 9C), or atrial and ventricular action potential durations (Fig. 9D). Furthermore, there are no observed differences between the atrial and ventricular conduction velocities in wild-type and *nkx2.5*$^{+/+}$;*nkx2.7*$^{-/-}$ embryos (Fig. 9E,F,I). In contrast, disruption of *nkx2.5* gene function affects multiple components of the action potential with significant slowing of the upstroke phase in both chambers (Fig. 9A-C), marked diminution of the maximum slope of the action potential upstroke (Fig. 9C), as well as a substantial prolongation of atrial action potential duration and accentuation of phase 4 depolarization in atrial CMs (Fig. 9A,D). Moreover, homozygous loss of *nkx2.5* function leads to severe slowing in action potential propagation, as demonstrated by closer spacing of the isochrones and significantly lower mean conduction velocities measured across both cardiac chambers (Fig. 9G-I). Interestingly, although there is failure of the normal specification of physiological AV delay in the hearts of *nkx2.5*$^{-/-}$;*nkx2.7*$^{+/+}$ embryos (Fig. 9K,L), there remain significant differences in action potential characteristics between the ventricle and atrium (Fig. 9J,K and Fig. S3A-C,E-G). Although the hearts from *nkx2.5*$^{+/+}$;*nkx2.7*$^{-/-}$ embryos did not exhibit any detectable electrophysiological phenotype (Fig. 9F), combined loss of function of both *nkx* homologs in *nkx2.5*$^{-/-}$;*nkx2.7*$^{-/-}$ embryos leads to complete loss of electrophysiological chamber identity and further slowing of the action potential upstroke phase in the atrium (Fig. 9A,C,J and Fig. S3D). The loss of action potential duration differences between chambers is also evident in *nkx2.5*$^{-/-}$;*nkx2.7*$^{-/-}$ embryos (Fig. 9D,K and Fig. S3H), including the emergence of a pacemaker phenotype in ventricular cells (Fig. 9B) and slowing of the conduction velocity (Fig. 9H,I,L). Interestingly, there are subtle, but significant, paradoxical effects on absolute atrial and ventricular conduction velocities in *nkx2.5*$^{-/-}$;*nkx2.7*$^{-/-}$ when compared with *nkx2.5*$^{-/-}$;*nkx2.7*$^{+/+}$ embryos. In the atrium, the *nkx2.5*$^{-/-}$;*nkx2.7*$^{-/-}$ embryos exhibit even slower conduction than the

Development (2018) 145, dev161497. doi:10.1242/dev.161497

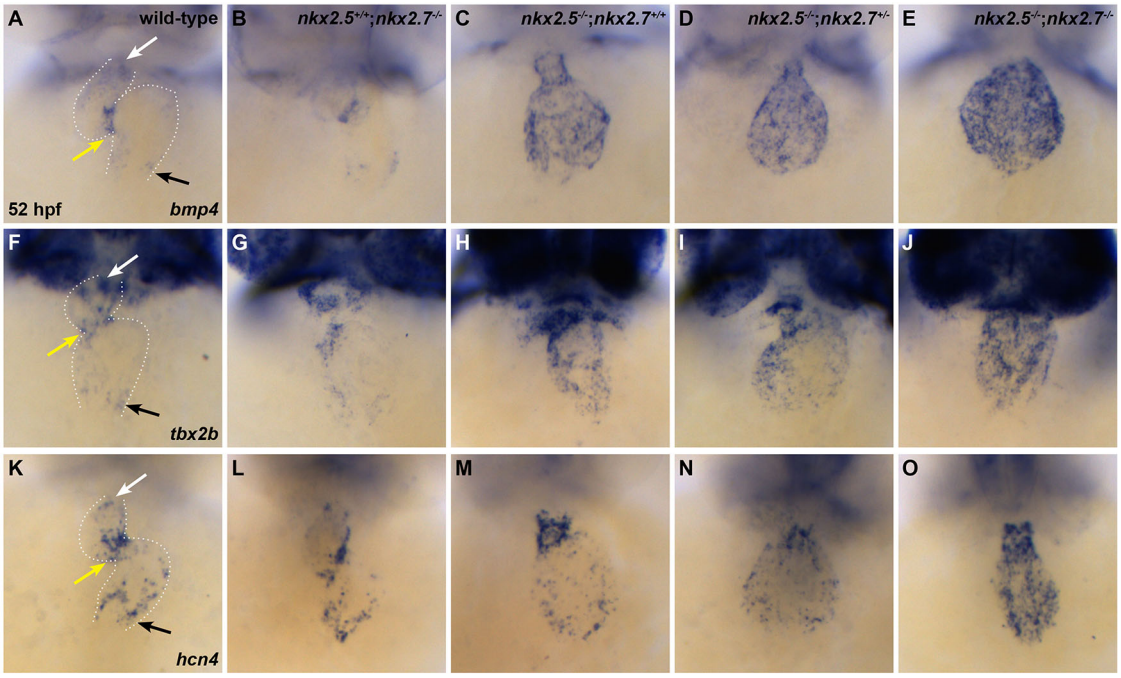

Fig. 7. Nkx genes regulate SAN markers. (A-O) Ventral view, anterior towards the top, at 52 hpf. Dotted white lines illustrate the cardiac silhouettes. *In situ* hybridization for *bmp4* (A-E), *tbx2b* (F-J) and *hcn4* (K-O). Expression of *bmp4* is restricted to the OFT (white arrow), AVC (yellow arrow) and IFT (black arrow) in wild-type (n=7/7) (A) and $nkx2.5^{+/+};nkx2.7^{-/-}$ (n=4/4) (B) embryos. However, its expression is expanded throughout the cardiac chambers in $nkx2.5^{-/-};nkx2.7^{+/+}$ (n=3/4) (C), $nkx2.5^{-/-};nkx2.7^{+/-}$ (n=3/3) (D) and $nkx2.5^{-/-};nkx2.7^{-/-}$ (n=3/3) (E) embryos. Similar findings are observed in the wild-type (n=6/7) (F), $nkx2.5^{+/+};nkx2.7^{-/-}$ (n=3/4) (G), $nkx2.5^{-/-};nkx2.7^{+/+}$ (n=3/3) (H), $nkx2.5^{-/-};nkx2.7^{+/-}$ (n=2/2) (I) and $nkx2.5^{-/-};nkx2.7^{-/-}$ (n=2/2) (J) embryos using the *tbx2b* probe, and in wild-type (n=8/8) (K), $nkx2.5^{+/+};nkx2.7^{-/-}$ (n=5/6) (L), $nkx2.5^{-/-};nkx2.7^{+/+}$ (n=9/11) (M), $nkx2.5^{-/-};nkx2.7^{+/-}$ (n=3/3) (N) and $nkx2.5^{-/-};nkx2.7^{-/-}$ (n=3/3) (O) embryos using the *hcn4* probe.

$nkx2.5^{-/-};nkx2.7^{+/+}$ embryos. However, in the ventricle, there is an increase in the conduction velocity in the $nkx2.5^{-/-};nkx2.7^{-/-}$ embryos, although conduction remains markedly slowed and chamber identity is lost from an electrophysiological standpoint. Although these electrophysiological attributes of the *nkx* mutant embryos reflect severe defects in intercellular coupling, the individual CM properties exhibit a phenotype that is more advanced developmentally than that observed in the primitive heart tube. Altogether, these data highlight the independent regulation of discrete CM parameters throughout early cardiac development and chamber identity maintenance.

DISCUSSION

Together, these findings offer new insights into the roles of Nkx genes in SHF development, highlighting the differential regulation at the arterial and venous poles. We show that Nkx genes promote the establishment of the SHF CM progenitor pool and differentiation of this population at the OFT. Our studies also reveal that Nkx genes are

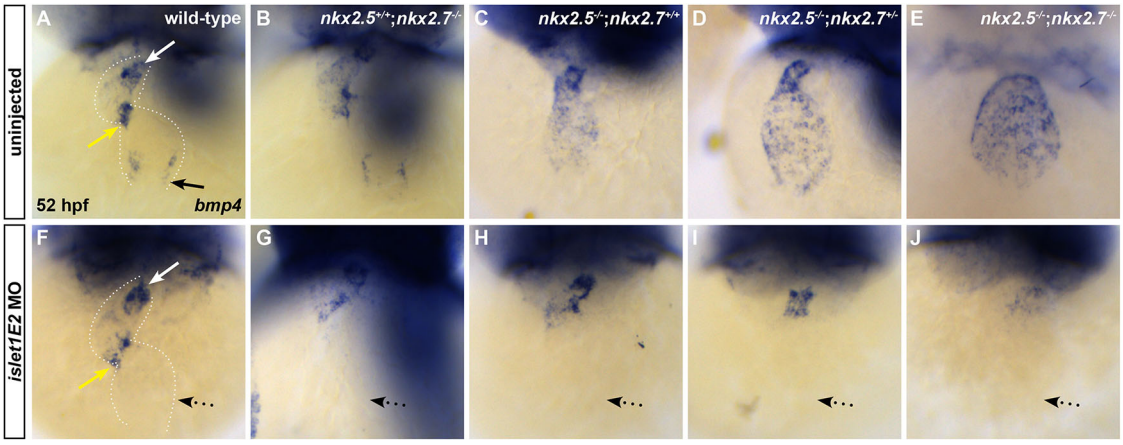

Fig. 8. *isl1* acts downstream of Nkx genes at the venous pole. (A-J) Ventral view, anterior towards the top, at 52 hpf. Dotted white lines illustrate the cardiac silhouettes. *In situ* hybridization for *bmp4* (A-J) in wild-type (A,F), $nkx2.5^{+/+};nkx2.7^{-/-}$ (B,G), $nkx2.5^{-/-};nkx2.7^{+/+}$ (C,H), $nkx2.5^{-/-};nkx2.7^{+/-}$ (D,I) and $nkx2.5^{-/-};nkx2.7^{-/-}$ (E,J) embryos. Inhibition of *isl1* expression using *islet1E2* MO in wild-type (n=4/4) (compare A with F) and $nkx2.5^{+/+};nkx2.7^{-/-}$ (n=4/4) (compare B and G) embryos leads to downregulation of *bmp4* expression specifically at the venous pole of the heart (black arrow) without affecting the AVC (yellow arrow) and OFT (white arrow) expression. In $nkx2.5^{-/-};nkx2.7^{+/+}$ (n=2/2), $nkx2.5^{-/-};nkx2.7^{+/-}$ (n=5/6) and $nkx2.5^{-/-};nkx2.7^{-/-}$ (n=3/3) embryos, *isl1* inhibition rescues the misregulation of *bmp4* expression in the atrium (dotted arrows), yet AVC and OFT expression patterns remain unchanged (compare C-E with H-J).

Development (2018) 145, dev161497. doi:10.1242/dev.161497

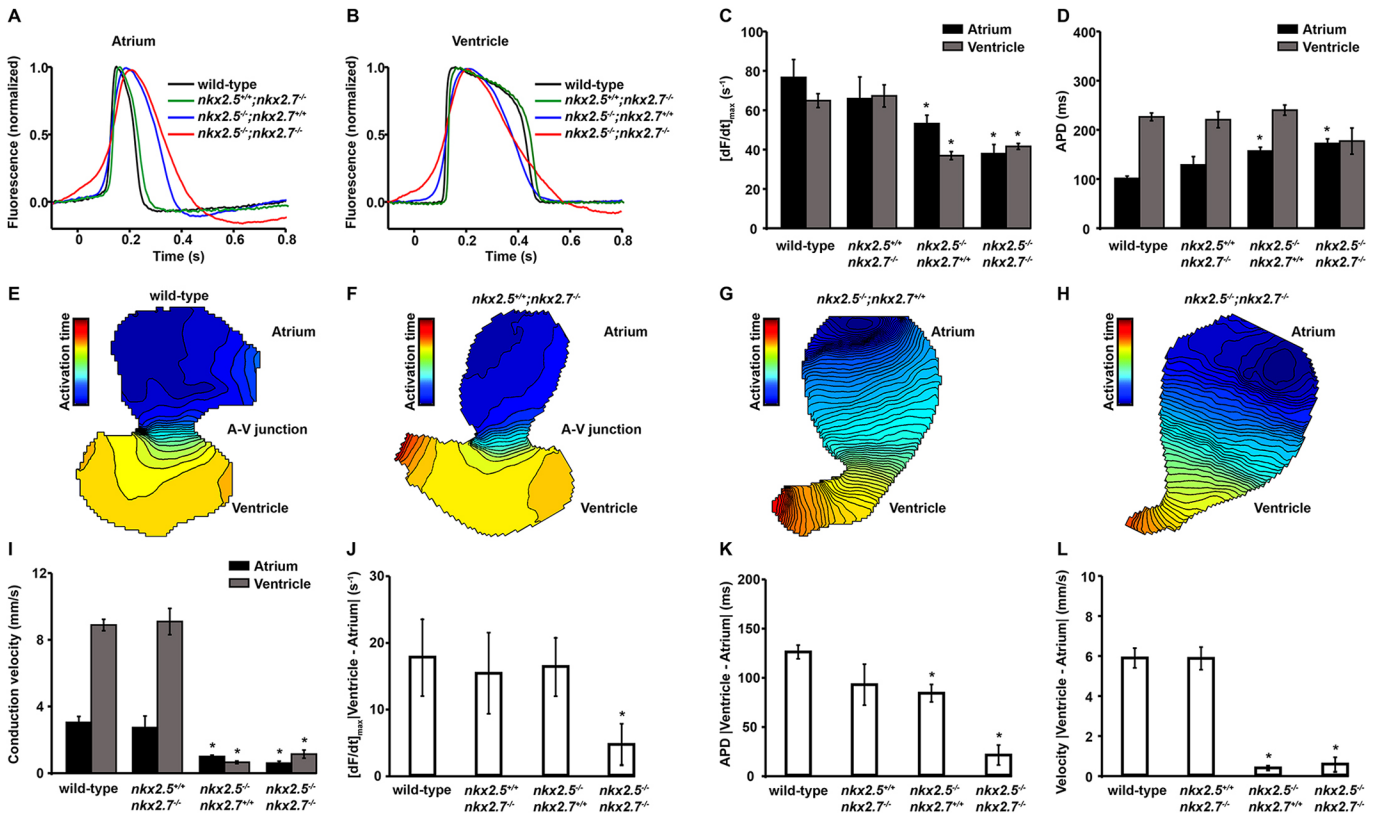

Fig. 9. Nkx genes regulate electrophysiological patterning. (A,B) Representative atrial (A) and ventricular (B) action potentials showing the time courses of cellular depolarization and repolarization in wild-type, *nkx2.5*$^{+/+}$;*nkx2.7*$^{-/-}$, *nkx2.5*$^{-/-}$;*nkx2.7*$^{+/+}$ and *nkx2.5*$^{-/-}$;*nkx2.7*$^{-/-}$ hearts. (C) Mean maximum slope of the atrial and ventricular action potentials measured as the maximum of the time derivative of the action potential upstroke phase, $[dF/dt]_{max}$, in wild-type, *nkx2.5*$^{+/+}$;*nkx2.7*$^{-/-}$, *nkx2.5*$^{-/-}$;*nkx2.7*$^{+/+}$ and *nkx2.5*$^{-/-}$;*nkx2.7*$^{-/-}$ hearts. (D) Action potential duration (APD) in wild-type, *nkx2.5*$^{+/+}$;*nkx2.7*$^{-/-}$, *nkx2.5*$^{-/-}$;*nkx2.7*$^{+/+}$ and *nkx2.5*$^{-/-}$;*nkx2.7*$^{-/-}$ hearts. (E-H) Representative isochronal maps illustrating the positions of the depolarizing wave front in 5 ms time intervals for wild-type (E), *nkx2.5*$^{+/+}$;*nkx2.7*$^{-/-}$ (F), *nkx2.5*$^{-/-}$;*nkx2.7*$^{+/+}$ (G) and *nkx2.5*$^{-/-}$;*nkx2.7*$^{-/-}$ (H) hearts. (I) Mean atrial and ventricular action potential propagation velocities in wild-type, *nkx2.5*$^{+/+}$;*nkx2.7*$^{-/-}$, *nkx2.5*$^{-/-}$;*nkx2.7*$^{+/+}$ and *nkx2.5*$^{-/-}$;*nkx2.7*$^{-/-}$ hearts. (J-L) Absolute differences in the maximum slope of the upstroke phase, $[dF/dt]_{max}$ (J), APD (K) and the conduction velocity (L) between the ventricle and the atrium in wild-type, *nkx2.5*$^{+/+}$;*nkx2.7*$^{-/-}$, *nkx2.5*$^{-/-}$;*nkx2.7*$^{+/+}$ and *nkx2.5*$^{-/-}$;*nkx2.7*$^{-/-}$ hearts. Student's *t*-test was used to determine statistical significance. The mean and s.e.m. of each data set are shown (*P<0.05) for wild-type (n=5), *nkx2.5*$^{+/+}$;*nkx2.7*$^{-/-}$ (n=5), *nkx2.5*$^{-/-}$;*nkx2.7*$^{+/+}$ (n=6) and *nkx2.5*$^{-/-}$;*nkx2.7*$^{-/-}$ (n=3) hearts.

essential for the proper patterning of the venous pole by regulating the maintenance of working myocardial properties through repression of *isl1*. Following the loss of *Nkx* gene function, the entire myocardium adopts an Isl1^{+} identity associated with activation of the SAN genes *bmp4*, *tbx2b, hcn4* and *shox2*. Misregulation of these SAN genes is associated with electrophysiological evidence of expansion of the pacemaker phenotype across both chambers, with cellular characteristics suggesting diminished sodium channel availability at the membranes, features of calcium-dependent action potentials, and diastolic phase 4 potentials. Together, our findings implicate Nkx genes in combinatorial roles for anterior-posterior patterning of chamber identity, regional integration of FHF and SHF territories, and maturation of discrete cassettes of physiological CM differentiation within the heart tube. Moreover, these cellular abnormalities induced by the loss of Nkx gene function in the two-chambered zebrafish heart offer a potential window into the morphological and conduction system defects in individuals with CHD that harbor *NKX2-5* mutations.

Through illustration of the differential functions of Nkx factors in the aSHF and pSHF, our studies complement and extend work in other model organisms. Previous studies have revealed a role for *Nkx2-5* in limiting cardiac progenitor specification and favoring SHF proliferation (Prall et al., 2007). Yet in zebrafish, early specification of SHF progenitors appears normal given the expression patterns of *nkx2.5*, *nkx2.7*, *hand2* (Targoff et al. 2013) and *isl1* (Fig. 5F-I) in *nkx* mutant embryos. However, *nkx2.5* has been shown to regulate SHF progenitor proliferation at the proximal OFT via *ltbp3* (Guner-Ataman et al., 2013). Through detailed dissection of the proliferative potential of the proximal and distal OFT progenitors, our results further elucidate the role that Nkx genes play in limiting the aSHF-derived CM population by regulating the timing of progenitor differentiation at the arterial pole. In view of studies illuminating a common progenitor of heart and head muscle derivatives in other models (Harel et al., 2012; Lescroart et al., 2015, 2010; Nagelberg et al., 2015; Wang et al., 2013), we postulate that aSHF progenitors could also adopt a head muscle fate in the absence of Nkx gene function. Future experiments would be required to test this hypothesis, which may offer additional insights into the diminished late-differentiating cells at the OFT of *nkx* mutant embryos. Taken together, although other mechanisms may play a role, our findings highlight a novel function of Nkx genes in establishing an aSHF progenitor pool necessary to assemble an arterial pole of the proper size and morphology.

Our data also illustrates that, in the absence of *nkx2.5*, the atrial myocardium adopts a venous pole identity characterized by misexpression of *isl1* and SAN genes associated with failure of specification of the cardiac conduction system (CCS) tissue at the AV boundary. Further graded expansion of this abnormal CM differentiation, including manifestation of increased cellular

Development (2018) 145, dev161497. doi:10.1242/dev.161497

automaticity and pacemaker-like behaviors throughout the entire ventricle, is observed following the combinatorial loss of *nkx2.5* and *nkx2.7*. Knockdown of *isl1* is sufficient to rescue the effects of *nkx* mutations on SAN gene expression, suggesting that Isl1 repression by Nkx genes patterns the venous pole of the heart and delineates the specialized CCS tissue. However, the molecular mechanisms by which Nkx genes control IFT development through refinement of *isl1* expression have yet to be determined. Specifically, the role of *bmp4* in establishing electrophysiological CM characteristics requires further investigation. Yet our results offer a potential explanation for the electrophysiological malfunction associated with the loss of fast-conducting properties and defects in specification of the ventricular conduction system lineage in *Nkx2-5*-deficient models (Moskowitz et al., 2007; Pashmforoush et al., 2004). Furthermore, we propose that the pivotal role for *nkx* genes in establishing a venous pole phenotype and SAN identity could explain progressive AV conduction defects into adulthood that are exhibited in individuals with *NKX2-5* mutations (Jay et al., 2003).

We have previously shown that ventricular CMs transdifferentiate into atrial CMs, demonstrating plasticity of the differentiated myocardium in *nkx* mutant embryos (Targoff et al., 2013). It is possible that flexibility of the differentiated CMs results in sarcomeric rearrangement that allows for fate transformation in the *nkx2.5*$^{-/-}$;*nkx2.7*$^{-/-}$ embryos. In support of this concept, a recent report demonstrates that ablation of ventricular CMs in the zebrafish embryos leads to atrial-to-ventricular transdifferentiation with associated sarcomeric restructuring (Zhang et al., 2013). Our electrophysiological studies further substantiate this hypothesis through their demonstration that graded loss of *nkx* alleles regulates multiple elements of the functional identity of the atrial and ventricular myocardium. Although atrial and ventricular action potential features and conduction properties are distinct in wild-type, *nkx2.5*$^{+/+}$;*nkx2.7*$^{-/-}$ and *nkx2.5*$^{-/-}$;*nkx2.7*$^{+/+}$ hearts, each of the individual null alleles exhibits discrete effects on resting membrane potentials, CM activation, action potential morphology and conduction velocity. Moreover, the electrophysiological differences between atrial and ventricular CMs are completely abolished in *nkx2.5*$^{-/-}$;*nkx2.7*$^{-/-}$ embryos. Despite these findings, there are discordances in the effects of individual genes on electrophysiology in the atrium and ventricle that implicate additional regulatory partners in the specification of the complex regional electrical function necessary for a vertebrate heart.

Taken together, these studies on the functions of Nkx genes in the aSHF and pSHF highlight important concepts in our understanding of CM differentiation. Changes in the expression of individual transcription factors, signaling molecules and ion channels reveal discrete physiological modules and can remodel nuanced functional characteristics in CMs. Given this malleability, the notion of a stable differentiated state does not fully reflect the resolution of modern cellular biology, which has revealed phenotypes that are a result of combinations of discrete and overlapping protein repertoires. These data parallel *in vitro* studies in iPS-derived differentiated cell types. Despite a physiological resemblance to mature CMs, these populations demonstrate remarkable cellular heterogeneity in detailed electrophysiological phenotypes and transcriptional profiles that more closely resemble one of the parent fibroblast than of the CM being studied. Our data suggest that individual proteins may be sufficient and necessary to induce and maintain plastic states where the regenerative potential in the heart might be realized. Thus, it would be valuable to address the fundamental nature of cardiomyocyte differentiation at the level of individual physiologic functions in order to obtain a better understanding of the different potential for cardiac regeneration between zebrafish and higher vertebrates.

MATERIALS AND METHODS

Zebrafish mutations and transgenes

We used zebrafish carrying the following previously described mutations and transgenes: *nkx2.5*^{vu179} (Targoff et al., 2013), *nkx2.7*^{vu413} (Targoff et al., 2013), *Tg(-5.1myl7:nDsRed2)*^{f2} (Mably et al., 2003), *Tg(myl7:EGFP)*^{twu277} (Huang et al., 2003), *Tg(nkx2.5:ZsYellow)*^{fb7} (Zhou et al., 2011) and *Tg(hsp70l:nkx2.5-EGFP)* (Targoff et al., 2013). All zebrafish work followed Institutional Animal Care and Use Committee-approved protocols.

Injection

Embryos were injected at the one-cell stage with 6 ng of the validated morpholino (MO) *islet1E2* (5′-TTAATCTGCGTTACCTGATGTAGTC-3′) (Hutchinson and Eisen, 2006). Uninjected sibling embryos were processed as controls.

Heat shock conditions

Embryos from outcrosses of fish carrying *Tg(hsp70l:nkx2.5-EGFP)* were maintained at 28.5°C and exposed to heat shock at 37°C at desired stages (21 somites to 24 somites). To implement heat shock, 50 embryos were placed in 2.5 ml of embryo medium in a 35 mm Petri dish on top of a covered heat block for 1 h. Three hours after the initiation of heat shock, transgenic embryos were identified by visualization of ubiquitous EGFP expression. Non-transgenic sibling embryos exposed to heat shock served as controls.

Depigmentation of embryos

When necessary, embryos were depigmented after overnight fixation in 4% paraformaldehyde at 4°C. They were washed twice in PBT (PBS-0.1% Tween) then incubated in 3% H_2O_2, 0.5% KOH and 0.1% Tween for 8 min at 26 h post fertilization (hpf) and 18 min at 52 hpf. Subsequently, the embryos were washed twice again in PBT and stored in methanol at −20°C.

In situ hybridization

We performed whole-mount *in situ* hybridization as previously described (Yelon et al., 1999) for *mef2cb* (ZDB-GENE-040901-7), *isl1* (ZDB-GENE-980526-112), *bmp4* (ZDB-GENE-980528-2059), *tbx2b* (ZDB-GENE-990726-27), *hcn4* (ZDB-GENE-050420-360) and *shox2* (ZDB-GENE-040426-1457).

Immunofluorescence

Whole-mount double immunofluorescence was conducted using a protocol described previously (Alexander et al., 1998) for the following primary antibodies: anti-Islet1/2 (1:50; 39.4D5, Developmental Studies Hybridoma Bank), anti-atrial myosin heavy chain (1:20; S46, Developmental Studies Hybridoma Bank), anti-RCFP (1:50; Clontech, 632475) and anti-GFP (1:100; Life Technologies, A11122). When employing the following primary antibodies, anti-Eln2 (1:500; Miao et al., 2007) and anti-sarcomeric myosin heavy chain (1:20; MF20, Developmental Studies Hybridoma Bank), another published protocol was used (Zhou et al., 2011). The following secondary antibodies were employed: goat anti-mouse IgG2b Alexa Fluor 488 or 568, goat anti-mouse IgG1 Alexa Fluor 488 or 568, goat anti-mouse IgG2a Alexa Fluor 488, goat anti-rabbit IgG Alexa Fluor 488 or 568, and goat anti-mouse IgG Cy5 (all at 1:200; Invitrogen).

Proliferation assay

Cardiomyocyte proliferation in embryos expressing *Tg(-5.1myl7:nDsRed2)*^{f2} or *Tg(nkx2.5:ZsYellow)*^{fb7} was assessed using the Click-iT EdU Imaging Kit (Life Technologies) with reported protocols (Cheesman et al., 2011; Mahler et al., 2010; Schindler et al., 2014). Following EdU incubation for 30 min on ice, embryos were chased for 24 h. Embryos were then fixed in 2% formaldehyde, washed once in PBS and washed twice in PBS-0.2% saponin. Subsequently, immunostaining was performed as described above followed by the Click-iT staining reaction. EdU^{+} ZsYellow^{+} MF20$^{+/-}$ and EdU^{+} DsRed^{+} MF20^{-} cells were counted using ImageJ software, going through all *z*-stacks. We calculated the proliferation indices as the percentage

of cells that incorporated EdU. Student's *t*-test (homoscedastic, two-tailed distribution) determined statistical significance between the means of cell number data sets.

Imaging

Images were captured with a Zeiss M2Bio microscope and a Zeiss AxioCam digital camera, prior to processing with Zeiss AxioVision and Adobe Creative Suite software. Confocal imaging was performed with a Nikon A1R MP confocal microscope and *z*-stacks were analyzed with ImageJ.

Developmental timing assay and cell counting

For the developmental timing assay, embryos carrying *Tg(-5.1myl7:nDsRed2)*^{f2} and *Tg(myl7:EGFP)*^{twu277} were fixed at 52 hpf for 1 h in 1% formaldehyde, washed once in PBS, washed three times in PBS-0.2% saponin, deyolked and flat-mounted. Newly differentiated CMs were identified as green, but not red cells (EGFP^{+} DsRed^{-} CMs) and were counted on *z*-stacks using ImageJ software. To count Isl1^{+} cells, we performed immunostaining for Isl1 and S46 (as described above) and quantified individual CMs that were positive for Isl1 using ImageJ software on reconstructed *z*-stacks. Student's *t*-test (homoscedastic, two-tailed distribution) determined statistical significance between the means of cell number data sets.

Genotyping

PCR genotyping was performed on genomic DNA extracted from individual embryos following *in situ* hybridization, immunofluorescence or live imaging. Detection of *nkx2.5*^{vu179} was performed using primers 5′-CAAACTCACCTCCACACAGG-3′ and 5′-TTACCATCCCGAACCA-AAAC-3′ to generate a 144 bp fragment. Digestion of the mutant PCR product with *Hin*f1 generates 30 bp and 114 bp fragments. Analysis of *nkx2.5*^{vu179} in embryos carrying *Tg(hsp70l:nkx2.5-EGFP)* was performed as previously described (George et al., 2015). Detection of *nkx2.7*^{vu413} was executed using primers 5′-TTGTTGCAAATGGACACGTT-3′ and 5′-G-GAGTGTCTCGCCGTTTTTA-3′ to generate a 158 bp fragment. Digestion of the mutant PCR product with *Mse*I creates 28 bp and 130 bp fragments.

Optical mapping

Embryonic zebrafish hearts were isolated at 72 hpf and stained with the transmembrane potential-sensitive dye, di-8-ANEPPS (Invitrogen), to measure action potentials using high-speed optical mapping as previously described (Mosimann et al., 2015; Panáková et al., 2010). Fluorescence intensities were recorded with a high-speed CCD camera (CardioCCD-SMQ, Redshirt Imaging) at 2000 frames per second. Activation times were determined as the times at which action potentials reached 50% of their amplitude during the depolarization phase at every location. This criterion for defining electrical activation was found in computer simulations to correlate with the time at which the maximum depolarizing Na^{+} current occurs during propagation (Fast and Kleber, 1995). Action potentials were temporally (800 Hz low-pass cutoff) and spatially (3×3 pixel average) filtered to enhance signal-to-noise ratios. To quantify the slope of the action potential upstroke phase, the maximum time derivative of the normalized action potential, $[dF/dt]_{max}$, was calculated. Action potential duration (APD) was defined as the absolute time difference between the decay phase and the upstroke phase of the local action potential at 50% depolarization. By fitting a second-order polynomial hypersurface to the three-dimensional image plane-activation time relationship, conduction velocity vectors were subsequently derived using an established algorithm (Bayly et al., 1998) with custom scripts. Conduction velocity vector fields were estimated from the local action potentials (Panáková et al., 2010). All electrophysiological measurements were averaged across the relevant anatomic segments for each heart.

Acknowledgements

We are grateful to Joshua Barber for expert zebrafish care and members of the Targoff Laboratory for their constructive input. We appreciate the critical reading of the manuscript by Lilianna Solnica-Krezel and Joshua S. Waxman. We also thank C. Geoffrey Burns and Caroline E. Burns for sharing the *Tg(nkx2.5:ZsYellow)* line.

Competing interests

S.C. is currently a consultant for Pairnomix, but the work presented in this paper has no connection with this company.

Author contributions

Conceptualization: S.C., K.L.T.; Methodology: S.C., C.A.M., K.L.T.; Validation: S.C., C.d.S.-T., A.A.W., C.A.M., K.L.T.; Formal analysis: S.C., C.d.S.-T., V.G., A.A.W., S.K., C.A.M., K.L.T.; Investigation: S.C., C.d.S.-T., V.G., A.A.W., S.K., C.A.M., K.L.T.; Resources: S.C., C.A.M., K.L.T.; Data curation: S.C., C.d.S.-T., V.G., A.A.W., S.K.; Writing - original draft: S.C., A.A.W., C.A.M., K.L.T.; Writing - review & editing: C.A.M., K.L.T.; Visualization: K.L.T.; Supervision: C.A.M., K.L.T.; Project administration: K.L.T.; Funding acquisition: C.A.M., K.L.T.

Funding

This work was supported by grants from the National Institutes of Health (K12HD043389, K08HL088002 and R01HL131438 to K.L.T., and R24OD017870 to C.A.M.] and the Burroughs Wellcome Fund [IRSA to C.A.M.]. Deposited in PMC for release after 12 months.

Supplementary information

Supplementary information available online at
http://dev.biologists.org/lookup/doi/10.1242/dev.161497.supplemental

References

Abou Hassan, O. K., Fahed, A. C., Batrawi, M., Arabi, M., Refaat, M. M., DePalma, S. R., Seidman, J. G., Seidman, C. E., Bitar, F. F. and Nemer, G. M. (2015). NKX2-5 mutations in an inbred consanguineous population: genetic and phenotypic diversity. *Sci. Rep.* **5**, 8848.

Alexander, J., Stainier, D. Y. R. and Yelon, D. (1998). Screening mosaic F1 females for mutations affecting zebrafish heart induction and patterning. *Dev. Genet.* **22**, 288-299.

Arrenberg, A. B., Stainier, D. Y. R., Baier, H. and Huisken, J. (2010). Optogenetic control of cardiac function. *Science* **330**, 971-974.

Azpiazu, N. and Frasch, M. (1993). tinman and bagpipe: two homeo box genes that determine cell fates in the dorsal mesoderm of Drosophila. *Genes Dev.* **7**, 1325-1340.

Barth, J. L., Clark, C. D., Fresco, V. M., Knoll, E. P., Lee, B., Argraves, W. S. and Lee, K.-H. (2010). Jarid2 is among a set of genes differentially regulated by Nkx2.5 during outflow tract morphogenesis. *Dev. Dyn.* **239**, 2024-2033.

Bayly, P. V., KenKnight, B. H., Rogers, J. M., Hillsley, R. E., Ideker, R. E. and Smith, W. M. (1998). Estimation of conduction velocity vector fields from epicardial mapping data. *IEEE Trans. Biomed. Eng.* **45**, 563-571.

Benson, D. W., Silberbach, G. M., Kavanaugh-McHugh, A., Cottrill, C., Zhang, Y., Riggs, S., Smalls, O., Johnson, M. C., Watson, M. S., Seidman, J. G. et al. (1999). Mutations in the cardiac transcription factor NKX2.5 affect diverse cardiac developmental pathways. *J. Clin. Invest.* **104**, 1567-1573.

Blaschke, R. J., Hahurij, N. D., Kuijper, S., Just, S., Wisse, L. J., Deissler, K., Maxelon, T., Anastassiadis, K., Spitzer, J., Hardt, S. E. et al. (2007). Targeted mutation reveals essential functions of the homeodomain transcription factor Shox2 in sinoatrial and pacemaking development. *Circulation* **115**, 1830-1838.

Bodmer, R. (1993). The gene tinman is required for specification of the heart and visceral muscles in Drosophila. *Development* **118**, 719-729.

Bouveret, R., Waardenberg, A. J., Schonrock, N., Ramialison, M., Doan, T., de Jong, D., Bondue, A., Kaur, G., Mohamed, S., Fonoudi, H. et al. (2015). NKX2-5 mutations causative for congenital heart disease retain functionality and are directed to hundreds of targets. *Elife* **4**, e06942.

Brade, T., Gessert, S., Kühl, M. and Pandur, P. (2007). The amphibian second heart field: Xenopus islet-1 is required for cardiovascular development. *Dev. Biol.* **311**, 297-310.

Briggs, L. E., Takeda, M., Cuadra, A. E., Wakimoto, H., Marks, M. H., Walker, A. J., Seki, T., Oh, S. P., Lu, J. T., Sumners, C. et al. (2008). Perinatal loss of Nkx2-5 results in rapid conduction and contraction defects. *Circ. Res.* **103**, 580-590.

Bruneau, B. G. (2008). The developmental genetics of congenital heart disease. *Nature* **451**, 943-948.

Buckingham, M., Meilhac, S. and Zaffran, S. (2005). Building the mammalian heart from two sources of myocardial cells. *Nat. Rev. Genet.* **6**, 826-837.

Cai, C.-L., Liang, X., Shi, Y., Chu, P.-H., Pfaff, S. L., Chen, J. and Evans, S. (2003). Isl1 identifies a cardiac progenitor population that proliferates prior to differentiation and contributes a majority of cells to the heart. *Dev. Cell* **5**, 877-889.

Cambier, L., Plate, M., Sucov, H. M. and Pashmforoush, M. (2014). Nkx2-5 regulates cardiac growth through modulation of Wnt signaling by R-spondin3. *Development* **141**, 2959-2971.

Cheesman, S. E., Neal, J. T., Mittge, E., Seredick, B. M. and Guillemin, K. (2011). Epithelial cell proliferation in the developing zebrafish intestine is regulated by the Wnt pathway and microbial signaling via Myd88. *Proc. Natl. Acad. Sci. USA* **108** Suppl. 1, 4570-4577.

Chi, N. C., Shaw, R. M., Jungblut, B., Huisken, J., Ferrer, T., Arnaout, R., Scott, I., Beis, D., Xiao, T., Baier, H. et al. (2008). Genetic and physiologic dissection of the vertebrate cardiac conduction system. *PLoS Biol.* **6**, e109.
Chung, I.-M. and Rajakumar, G. (2016). Genetics of congenital heart defects: the NKX2-5 gene, a key player. *Genes* **7**, 6.
Clark, C. D., Zhang, B., Lee, B., Evans, S. I., Lassar, A. B. and Lee, K.-H. (2013). Evolutionary conservation of Nkx2.5 autoregulation in the second heart field. *Dev. Biol.* **374**, 198-209.
D'Amico, L., Scott, I. C., Jungblut, B. and Stainier, D. Y. R. (2007). A mutation in zebrafish hmgcr1b reveals a role for isoprenoids in vertebrate heart-tube formation. *Curr. Biol.* **17**, 252-259.
de Pater, E., Clijsters, L., Marques, S. R., Lin, Y.-F., Garavito-Aguilar, Z. V., Yelon, D. and Bakkers, J. (2009). Distinct phases of cardiomyocyte differentiation regulate growth of the zebrafish heart. *Development* **136**, 1633-1641.
Dominguez, J. N., Meilhac, S. M., Bland, Y. S., Buckingham, M. E. and Brown, N. A. (2012). Asymmetric fate of the posterior part of the second heart field results in unexpected left/right contributions to both poles of the heart. *Circ. Res.* **111**, 1323-1335.
Dorn, T., Goedel, A., Lam, J. T., Haas, J., Tian, Q., Herrmann, F., Bundschu, K., Dobreva, G., Schiemann, M., Dirschinger, R. et al. (2014). Direct Nkx2-5 transcriptional repression of Isl1 controls cardiomyocyte subtype identity. *Stem Cells* **33**, 1113-1129.
Dyer, L. A. and Kirby, M. L. (2009). The role of secondary heart field in cardiac development. *Dev. Biol.* **336**, 137-144.
Elliott, D. A., Kirk, E. P., Yeoh, T., Chandar, S., McKenzie, F., Taylor, P., Grossfeld, P., Fatkin, D., Jones, O., Hayes, P. et al. (2003). Cardiac homeobox gene NKX2-5 mutations and congenital heart disease: associations with atrial septal defect and hypoplastic left heart syndrome. *J. Am. Coll. Cardiol.* **41**, 2072-2076.
Espinoza-Lewis, R. A., Yu, L., He, F., Liu, H., Tang, R., Shi, J., Sun, X., Martin, J. F., Wang, D., Yang, J. et al. (2009). Shox2 is essential for the differentiation of cardiac pacemaker cells by repressing Nkx2-5. *Dev. Biol.* **327**, 376-385.
Espinoza-Lewis, R. A., Liu, H., Sun, C., Chen, C., Jiao, K. and Chen, Y. P. (2011). Ectopic expression of Nkx2.5 suppresses the formation of the sinoatrial node in mice. *Dev. Biol.* **356**, 359-369.
Fast, V. G. and Kleber, A. G. (1995). Cardiac tissue geometry as a determinant of unidirectional conduction block: assessment of microscopic excitation spread by optical mapping in patterned cell cultures and in a computer model. *Cardiovasc. Res.* **29**, 697-707.
Galli, D., Dominguez, J. N., Zaffran, S., Munk, A., Brown, N. A. and Buckingham, M. E. (2008). Atrial myocardium derives from the posterior region of the second heart field, which acquires left-right identity as Pitx2c is expressed. *Development* **135**, 1157-1167.
Gelb, B. D. and Chung, W. K. (2014). Complex genetics and the etiology of human congenital heart disease. *Cold Spring Harb. Perspect. Med.* **4**, a013953.
George, V., Colombo, S. and Targoff, K. L. (2015). An early requirement for nkx2.5 ensures the first and second heart field ventricular identity and cardiac function into adulthood. *Dev. Biol.* **400**, 10-22.
Goddeeris, M. M., Rho, S., Petiet, A., Davenport, C. L., Johnson, G. A., Meyers, E. N. and Klingensmith, J. (2008). Intracardiac septation requires hedgehog-dependent cellular contributions from outside the heart. *Development* **135**, 1887-1895.
Goldmuntz, E., Geiger, E. and Benson, D. W. (2001). NKX2.5 mutations in patients with tetralogy of fallot. *Circulation* **104**, 2565-2568.
Grow, M. W. and Krieg, P. A. (1998). Tinman function is essential for vertebrate heart development: elimination of cardiac differentiation by dominant inhibitory mutants of the tinman-related genes, XNkx2-3 and XNkx2-5. *Dev. Biol.* **204**, 187-196.
Guner-Ataman, B., Paffett-Lugassy, N., Adams, M. S., Nevis, K. R., Jahangiri, L., Obregon, P., Kikuchi, K., Poss, K. D., Burns, C. E. and Burns, C. G. (2013). Zebrafish second heart field development relies on progenitor specification in anterior lateral plate mesoderm and nkx2.5 function. *Development* **140**, 1353-1363.
Gutierrez-Roelens, I., Sluysmans, T., Gewillig, M., Devriendt, K. and Vikkula, M. (2002). Progressive AV-block and anomalous venous return among cardiac anomalies associated with two novel missense mutations in the CSX/NKX2-5 gene. *Hum. Mutat.* **20**, 75-76.
Hami, D., Grimes, A. C., Tsai, H.-J. and Kirby, M. L. (2011). Zebrafish cardiac development requires a conserved secondary heart field. *Development* **138**, 2389-2398.
Harel, I., Maezawa, Y., Avraham, R., Rinon, A., Ma, H.-Y., Cross, J. W., Leviatan, N., Hegesh, J., Roy, A., Jacob-Hirsch, J. et al. (2012). Pharyngeal mesoderm regulatory network controls cardiac and head muscle morphogenesis. *Proc. Natl. Acad. Sci. USA* **109**, 18839-18844.
Hoffman, J. I. E. and Kaplan, S. (2002). The incidence of congenital heart disease. *J. Am. Coll. Cardiol.* **39**, 1890-1900.
Hoffman, J. I. E., Kaplan, S. and Liberthson, R. R. (2004). Prevalence of congenital heart disease. *Am. Heart J.* **147**, 425-439.
Hoffmann, A. D., Peterson, M. A., Friedland-Little, J. M., Anderson, S. A. and Moskowitz, I. P. (2009). sonic hedgehog is required in pulmonary endoderm for atrial septation. *Development* **136**, 1761-1770.
Hoffmann, S., Berger, I. M., Glaser, A., Bacon, C., Li, L., Gretz, N., Steinbeisser, H., Rottbauer, W., Just, S. and Rappold, G. (2013). Islet1 is a direct transcriptional target of the homeodomain transcription factor Shox2 and rescues the Shox2-mediated bradycardia. *Basic Res. Cardiol.* **108**, 339.
Hoffmann, A. D., Yang, X. H., Burnicka-Turek, O., Bosman, J. D., Ren, X., Steimle, J. D., Vokes, S. A., McMahon, A. P., Kalinichenko, V. V. and Moskowitz, I. P. (2014). Foxf genes integrate tbx5 and hedgehog pathways in the second heart field for cardiac septation. *PLoS Genet.* **10**, e1004604.
Huang, C.-J., Tu, C.-T., Hsiao, C.-D., Hsieh, F.-J. and Tsai, H.-J. (2003). Germ-line transmission of a myocardium-specific GFP transgene reveals critical regulatory elements in the cardiac myosin light chain 2 promoter of zebrafish. *Dev. Dyn.* **228**, 30-40.
Hutchinson, S. A. and Eisen, J. S. (2006). Islet1 and Islet2 have equivalent abilities to promote motoneuron formation and to specify motoneuron subtype identity. *Development* **133**, 2137-2147.
Hutson, M. R., Zeng, X. L., Kim, A. J., Antoon, E., Harward, S. and Kirby, M. L. (2010). Arterial pole progenitors interpret opposing FGF/BMP signals to proliferate or differentiate. *Development* **137**, 3001-3011.
Ikeda, Y., Hiroi, Y., Hosoda, T., Utsunomiya, T., Matsuo, S., Ito, T., Inoue, J., Sumiyoshi, T., Takano, H., Nagai, R. et al. (2002). Novel point mutation in the cardiac transcription factor CSX/NKX2.5 associated with congenital heart disease. *Circ. J.* **66**, 561-563.
Jahangiri, L., Sharpe, M., Novikov, N., Gonzalez-Rosa, J. M., Borikova, A., Nevis, K., Paffett-Lugassy, N., Zhao, L., Adams, M., Guner-Ataman, B. et al. (2016). The AP-1 transcription factor component Fosl2 potentiates the rate of myocardial differentiation from the zebrafish second heart field. *Development* **143**, 113-122.
Jay, P. Y., Berul, C. I., Tanaka, M., Ishii, M., Kurachi, Y. and Izumo, S. (2003). Cardiac conduction and arrhythmia: insights from Nkx2.5 mutations in mouse and humans. *Novartis Found. Symp.* **250**, 227-238; discussion 238-241, 276-229.
Jay, P. Y., Harris, B. S., Maguire, C. T., Buerger, A., Wakimoto, H., Tanaka, M., Kupershmidt, S., Roden, D. M., Schultheiss, T. M., O'Brien, T. X. et al. (2004). Nkx2-5 mutation causes anatomic hypoplasia of the cardiac conduction system. *J. Clin. Invest.* **113**, 1130-1137.
Lazic, S. and Scott, I. C. (2011). Mef2cb regulates late myocardial cell addition from a second heart field-like population of progenitors in zebrafish. *Dev. Biol.* **354**, 123-133.
Lee, K.-H., Xu, Q. and Breitbart, R. E. (1996). A new tinman-related gene, nkx2.7, anticipates the expression of nkx2.5 and nkx2.3 in zebrafish heart and pharyngeal endoderm. *Dev. Biol.* **180**, 722-731.
Lescroart, F., Kelly, R. G., Le Garrec, J.-F., Nicolas, J.-F., Meilhac, S. M. and Buckingham, M. (2010). Clonal analysis reveals common lineage relationships between head muscles and second heart field derivatives in the mouse embryo. *Development* **137**, 3269-3279.
Lescroart, F., Mohun, T., Meilhac, S. M., Bennett, M. and Buckingham, M. (2012). Lineage tree for the venous pole of the heart: clonal analysis clarifies controversial genealogy based on genetic tracing. *Circ. Res.* **111**, 1313-1322.
Lescroart, F., Hamou, W., Francou, A., Théveniau-Ruissy, M., Kelly, R. G. and Buckingham, M. (2015). Clonal analysis reveals a common origin between nonsomite-derived neck muscles and heart myocardium. *Proc. Natl. Acad. Sci. USA* **112**, 1446-1451.
Liang, X., Zhang, Q., Cattaneo, P., Zhuang, S., Gong, X., Spann, N. J., Jiang, C., Cao, X., Zhao, X., Zhang, X. et al. (2015). Transcription factor ISL1 is essential for pacemaker development and function. *J. Clin. Invest.* **125**, 3256-3268.
Loffredo, C. A. (2000). Epidemiology of cardiovascular malformations: prevalence and risk factors. *Am. J. Med. Genet.* **97**, 319-325.
Lyons, I., Parsons, L. M., Hartley, L., Li, R., Andrews, J. E., Robb, L. and Harvey, R. P. (1995). Myogenic and morphogenetic defects in the heart tubes of murine embryos lacking the homeo box gene Nkx2-5. *Genes Dev.* **9**, 1654-1666.
Mably, J. D., Mohideen, M. A., Burns, C. G., Chen, J.-N., Fishman, M. C. and Mohideen, M.-A. P. K. (2003). heart of glass regulates the concentric growth of the heart in zebrafish. *Curr. Biol.* **13**, 2138-2147.
Mahler, J., Filippi, A. and Driever, W. (2010). DeltaA/DeltaD regulate multiple and temporally distinct phases of notch signaling during dopaminergic neurogenesis in zebrafish. *J. Neurosci.* **30**, 16621-16635.
McElhinney, D. B., Geiger, E., Blinder, J., Benson, D. W. and Goldmuntz, E. (2003). NKX2.5 mutations in patients with congenital heart disease. *J. Am. Coll. Cardiol.* **42**, 1650-1655.
Miao, M., Bruce, A. E. E., Bhanji, T., Davis, E. C. and Keeley, F. W. (2007). Differential expression of two tropoelastin genes in zebrafish. *Matrix Biol.* **26**, 115-124.
Milan, D. J., Giokas, A. C., Serluca, F. C., Peterson, R. T. and MacRae, C. A. (2006). Notch1b and neuregulin are required for specification of central cardiac conduction tissue. *Development* **133**, 1125-1132.
Mommersteeg, M. T. M., Soufan, A. T., de Lange, F. J., van den Hoff, M. J., Anderson, R. H., Christoffels, V. M. and Moorman, A. F. (2006). Two distinct pools of mesenchyme contribute to the development of the atrial septum. *Circ. Res.* **99**, 351-353.
Mommersteeg, M. T. M., Brown, N. A., Prall, O. W. J., de Gier-de Vries, C., Harvey, R. P., Moorman, A. F. M. and Christoffels, V. M. (2007). Pitx2c and

Nkx2-5 are required for the formation and identity of the pulmonary myocardium. *Circ. Res.* **101**, 902-909.
Mosimann, C., Panáková, D., Werdich, A. A., Musso, G., Burger, A., Lawson, K. L., Carr, L. A., Nevis, K. R., Sabeh, M. K., Zhou, Y. et al. (2015). Chamber identity programs drive early functional partitioning of the heart. *Nat. Commun.* **6**, 8146.
Moskowitz, I. P. G., Kim, J. B., Moore, M. L., Wolf, C. M., Peterson, M. A., Shendure, J., Nobrega, M. A., Yokota, Y., Berul, C., Izumo, S. et al. (2007). A molecular pathway including Id2, Tbx5, and Nkx2-5 required for cardiac conduction system development. *Cell* **129**, 1365-1376.
Nagelberg, D., Wang, J., Su, R., Torres-Vázquez, J., Targoff, K. L., Poss, K. D. and Knaut, H. (2015). Origin, specification, and plasticity of the great vessels of the heart. *Curr. Biol.* **25**, 2099-2110.
Nakajima, Y. (2010). Second lineage of heart forming region provides new understanding of conotruncal heart defects. *Congenit. Anom.* **50**, 8-14.
Nakashima, Y., Ono, K., Yoshida, Y., Kojima, Y., Kita, T., Tanaka, M. and Kimura, T. (2009). The search for Nkx2-5-regulated genes using purified embryonic stem cell-derived cardiomyocytes with Nkx2-5 gene targeting. *Biochem. Biophys. Res. Commun.* **390**, 821-826.
Nakashima, Y., Yanez, D. A., Touma, M., Nakano, H., Jaroszewicz, A., Jordan, M. C., Pellegrini, M., Roos, K. P. and Nakano, A. (2014). Nkx2-5 suppresses the proliferation of atrial myocytes and conduction system. *Circ. Res.* **114**, 1103-1113.
Nemer, M. (2008). Genetic insights into normal and abnormal heart development. *Cardiovasc. Pathol.* **17**, 48-54.
Nevis, K., Obregon, P., Walsh, C., Guner-Ataman, B., Burns, C. G. and Burns, C. E. (2013). Tbx1 is required for second heart field proliferation in zebrafish. *Dev. Dyn.* **242**, 550-559.
Paffett-Lugassy, N., Novikov, N., Jeffrey, S., Abrial, M., Guner-Ataman, B., Sakthivel, S., Burns, C. E. and Burns, C. G. (2017). Unique developmental trajectories and genetic regulation of ventricular and outflow tract progenitors in the zebrafish second heart field. *Development* **144**, 4616-4624.
Panáková, D., Werdich, A. A. and Macrae, C. A. (2010). Wnt11 patterns a myocardial electrical gradient through regulation of the L-type Ca(2+) channel. *Nature* **466**, 874-878.
Pandur, P., Sirbu, I. O., Kühl, S. J., Philipp, M. and Kühl, M. (2013). Islet1-expressing cardiac progenitor cells: a comparison across species. *Dev. Genes Evol.* **223**, 117-129.
Pashmforoush, M., Lu, J. T., Chen, H., Amand, T. S., Kondo, R., Pradervand, S., Evans, S. M., Clark, B., Feramisco, J. R., Giles, W. et al. (2004). Nkx2-5 pathways and congenital heart disease; loss of ventricular myocyte lineage specification leads to progressive cardiomyopathy and complete heart block. *Cell* **117**, 373-386.
Payne, R. M., Johnson, M. C., Grant, J. W. and Strauss, A. W. (1995). Toward a molecular understanding of congenital heart disease. *Circulation* **91**, 494-504.
Pierpont, M. E., Basson, C. T., Benson, D. W., Jr, Gelb, B. D., Giglia, T. M., Goldmuntz, E., McGee, G., Sable, C. A., Srivastava, D., Webb, C. L. et al. (2007). Genetic basis for congenital heart defects: current knowledge: a scientific statement from the American Heart Association Congenital Cardiac Defects Committee, Council on Cardiovascular Disease in the Young: endorsed by the American Academy of Pediatrics. *Circulation* **115**, 3015-3038.
Prall, O. W. J., Menon, M. K., Solloway, M. J., Watanabe, Y., Zaffran, S., Bajolle, F., Biben, C., McBride, J. J., Robertson, B. R., Chaulet, H. et al. (2007). An Nkx2-5/Bmp2/Smad1 negative feedback loop controls heart progenitor specification and proliferation. *Cell* **128**, 947-959.
Rana, M. S., Theveniau-Ruissy, M., De Bono, C., Mesbah, K., Francou, A., Rammah, M., Dominguez, J. N., Roux, M., Laforest, B., Anderson, R. H. et al. (2014). Tbx1 coordinates addition of posterior second heart field progenitor cells to the arterial and venous poles of the heart. *Circ. Res.* **115**, 790-799.
Schindler, Y. L., Garske, K. M., Wang, J., Firulli, B. A., Firulli, A. B., Poss, K. D. and Yelon, D. (2014). Hand2 elevates cardiomyocyte production during zebrafish heart development and regeneration. *Development* **141**, 3112-3122.
Schott, J. J., Benson, D. W., Basson, C. T., Pease, W., Silberbach, G. M., Moak, J. P., Maron, B. J., Seidman, C. E. and Seidman, J. G. (1998). Congenital heart disease caused by mutations in the transcription factor NKX2-5. *Science* **281**, 108-111.
Snarr, B. S., O'Neal, J. L., Chintalapudi, M. R., Wirrig, E. E., Phelps, A. L., Kubalak, S. W. and Wessels, A. (2007a). Isl1 expression at the venous pole identifies a novel role for the second heart field in cardiac development. *Circ. Res.* **101**, 971-974.
Snarr, B. S., Wirrig, E. E., Phelps, A. L., Trusk, T. C. and Wessels, A. (2007b). A spatiotemporal evaluation of the contribution of the dorsal mesenchymal protrusion to cardiac development. *Dev. Dyn.* **236**, 1287-1294.
Srivastava, D. and Olson, E. N. (2000). A genetic blueprint for cardiac development. *Nature* **407**, 221-226.
Stanley, E. G., Biben, C., Elefanty, A., Barnett, L., Koentgen, F., Robb, L. and Harvey, R. P. (2002). Efficient Cre-mediated deletion in cardiac progenitor cells conferred by a 3′UTR-ires-Cre allele of the homeobox gene Nkx2-5. *Int. J. Dev. Biol.* **46**, 431-439.
Stevens, K. N., Hakonarson, H., Kim, C. E., Doevendans, P. A., Koeleman, B. P. C., Mital, S., Raue, J., Glessner, J. T., Coles, J. G., Moreno, V. et al. (2010). Common variation in ISL1 confers genetic susceptibility for human congenital heart disease. *PLoS ONE* **5**, e10855.
Stoyek, M. R., Croll, R. P. and Smith, F. M. (2015). Intrinsic and extrinsic innervation of the heart in zebrafish (Danio rerio). *J. Comp. Neurol.* **523**, 1683-1700.
Sun, Y., Liang, X., Najafi, N., Cass, M., Lin, L., Cai, C.-L., Chen, J. and Evans, S. M. (2007). Islet 1 is expressed in distinct cardiovascular lineages, including pacemaker and coronary vascular cells. *Dev. Biol.* **304**, 286-296.
Supino, P. G., Borer, J. S., Preibisz, J. and Bornstein, A. (2006). The epidemiology of valvular heart disease: a growing public health problem. *Heart Fail. Clin.* **2**, 379-393.
Tanaka, M., Wechsler, S. B., Lee, I. W., Yamasaki, N., Lawitts, J. A. and Izumo, S. (1999). Complex modular cis-acting elements regulate expression of the cardiac specifying homeobox gene Csx/Nkx2.5. *Development* **126**, 1439-1450.
Targoff, K. L., Schell, T. and Yelon, D. (2008). Nkx genes regulate heart tube extension and exert differential effects on ventricular and atrial cell number. *Dev. Biol.* **322**, 314-321.
Targoff, K. L., Colombo, S., George, V., Schell, T., Kim, S.-H., Solnica-Krezel, L. and Yelon, D. (2013). Nkx genes are essential for maintenance of ventricular identity. *Development* **140**, 4203-4213.
Tessadori, F., van Weerd, J. H., Burkhard, S. B., Verkerk, A. O., de Pater, E., Boukens, B. J., Vink, A., Christoffels, V. M. and Bakkers, J. (2012). Identification and functional characterization of cardiac pacemaker cells in zebrafish. *PLoS ONE* **7**, e47644.
Tirosh-Finkel, L., Zeisel, A., Brodt-Ivenshitz, M., Shamai, A., Yao, Z., Seger, R., Domany, E. and Tzahor, E. (2010). BMP-mediated inhibition of FGF signaling promotes cardiomyocyte differentiation of anterior heart field progenitors. *Development* **137**, 2989-3000.
Tu, C.-T., Yang, T.-C. and Tsai, H.-J. (2009). Nkx2.7 and Nkx2.5 function redundantly and are required for cardiac morphogenesis of zebrafish embryos. *PLoS ONE* **4**, e4249.
van den Berg, G., Abu-Issa, R., de Boer, B. A., Hutson, M. R., de Boer, P. A. J., Soufan, A. T., Ruijter, J. M., Kirby, M. L., van den Hoff, M. J. B. and Moorman, A. F. M. (2009). A caudal proliferating growth center contributes to both poles of the forming heart tube. *Circ. Res.* **104**, 179-188.
Vedantham, V., Galang, G., Evangelista, M., Deo, R. C. and Srivastava, D. (2015). RNA sequencing of mouse sinoatrial node reveals an upstream regulatory role for Islet-1 in cardiac pacemaker cells. *Circ. Res.* **116**, 797-803.
Vincent, S. D. and Buckingham, M. E. (2010). How to make a heart: the origin and regulation of cardiac progenitor cells. *Curr. Top. Dev. Biol.* **90**, 1-41.
Wang, W., Razy-Krajka, F., Siu, E., Ketcham, A. and Christiaen, L. (2013). NK4 antagonizes Tbx1/10 to promote cardiac versus pharyngeal muscle fate in the ascidian second heart field. *PLoS Biol.* **11**, e1001725.
Watanabe, Y., Zaffran, S., Kuroiwa, A., Higuchi, H., Ogura, T., Harvey, R. P., Kelly, R. G. and Buckingham, M. (2012). Fibroblast growth factor 10 gene regulation in the second heart field by Tbx1, Nkx2-5, and Islet1 reveals a genetic switch for down-regulation in the myocardium. *Proc. Natl. Acad. Sci. USA* **109**, 18273-18280.
Witzel, H. R., Jungblut, B., Choe, C. P., Crump, J. G., Braun, T. and Dobreva, G. (2012). The LIM protein Ajuba restricts the second heart field progenitor pool by regulating Isl1 activity. *Dev. Cell* **23**, 58-70.
Witzel, H. R., Cheedipudi, S., Gao, R., Stainier, D. Y. R. and Dobreva, G. D. (2017). Isl2b regulates anterior second heart field development in zebrafish. *Sci. Rep.* **7**, 41043.
Xie, L., Hoffmann, A. D., Burnicka-Turek, O., Friedland-Little, J. M., Zhang, K. and Moskowitz, I. P. (2012). Tbx5-hedgehog molecular networks are essential in the second heart field for atrial septation. *Dev. Cell* **23**, 280-291.
Ye, W., Wang, J., Song, Y., Yu, D., Sun, C., Liu, C., Chen, F., Zhang, Y., Wang, F., Harvey, R. P. et al. (2015). A common Shox2-Nkx2-5 antagonistic mechanism primes the pacemaker cell fate in the pulmonary vein myocardium and sinoatrial node. *Development* **142**, 2521-2532.
Yelon, D., Horne, S. A. and Stainier, D. Y. R. (1999). Restricted expression of cardiac myosin genes reveals regulated aspects of heart tube assembly in zebrafish. *Dev. Biol.* **214**, 23-37.
Zaffran, S., Kelly, R. G., Meilhac, S. M., Buckingham, M. E. and Brown, N. A. (2004). Right ventricular myocardium derives from the anterior heart field. *Circ. Res.* **95**, 261-268.
Zeng, X.-X. I. and Yelon, D. (2014). Cadm4 restricts the production of cardiac outflow tract progenitor cells. *Cell Rep.* **7**, 951-960.
Zhang, R., Han, P., Yang, H., Ouyang, K., Lee, D., Lin, Y.-F., Ocorr, K., Kang, G., Chen, J., Stainier, D. Y. R. et al. (2013). In vivo cardiac reprogramming contributes to zebrafish heart regeneration. *Nature* **498**, 497-501.
Zhang, L., Nomura-Kitabayashi, A., Sultana, N., Cai, W., Cai, X., Moon, A. M. and Cai, C.-L. (2014). Mesodermal Nkx2.5 is necessary and sufficient for early second heart field development. *Dev. Biol.* **390**, 68-79.
Zhou, Y., Cashman, T. J., Nevis, K. R., Obregon, P., Carney, S. A., Liu, Y., Gu, A., Mosimann, C., Sondalle, S., Peterson, R. E. et al. (2011). Latent TGF-beta binding protein 3 identifies a second heart field in zebrafish. *Nature* **474**, 645-648.